Stantec

Kivalina Airstrip Revetment Life and Alternative Analysis

Kivalina, Alaska

February 16, 2024

Prepared for:

Alaska Department of Transportation
and Public Facilities

Prepared by:

Stantec Consulting Services, Inc.

This document entitled Kivalina Airstrip Revetment Life and Alternative Analysis was prepared by Stantec Consulting Services Inc. ("Stantec") for the account of Alaska Department of Transportation and Public Facilities (the "Client"). Any reliance on this document by any third party is strictly prohibited. The material in it reflects Stantec's professional judgment in light of the scope, schedule and other limitations stated in the document and in the contract between Stantec and the Client. The opinions in the document are based on conditions and information existing at the time the document was published and do not take into account any subsequent changes. In preparing the document, Stantec did not verify information supplied to it by others. Any use which a third party makes of this document is the responsibility of such third party. Such third party agrees that Stantec shall not be responsible for costs or damages of any kind, if any, suffered by it or any other third party as a result of decisions made or actions taken based on this document.

Prepared by ____
(signature)

Arturo Jimenez Martinez, P.E.

Reviewed by ____
(signature)

Todd DeMunda, P.E.

Approved by Ryan Cooper
(signature)

Ryan Cooper

Table of Contents

LIST OF TABLES

LIST OF FIGURES

Executive Summary

Kivalina is a city located in northwestern Alaska, that sits at the southern end of a barrier island that separates the Kivalina Lagoon from the Chukchi Sea. The city has an airstrip with an armor stone revetment on the seaward side to protect it from waves associated with storms in the Chukchi Sea that are characteristics of the fall and winter. A sea ice cover develops in the Chukchi Sea in the late fall and stays through the winter and spring, preventing winter storms from generating waves that would otherwise impact the revetment. However, global warming is reducing the spatial coverage and temporal duration of the sea ice cover, increasing the exposure of the revetment and vulnerability of the airstrip.

The Alaska Department of Transportation and Public Facilities tasked Stantec Consulting Services Inc. with: 1) estimating the remaining useful life of the existing airstrip revetment (completed in 2019) considering the extended exposure to storms in the fall/winter expected to occur due to global warming, 2) identifying alternatives to extend the useful life of the airstrip in its current location, and 3) provide cost estimates of those alternatives to compare against the cost of relocating the airstrip. This report presents the analyses carried out to address the first two objectives of the study.

The study includes analysis of metocean data, prediction of offshore waves in an ice-free winter using machine learning techniques, discussion on shoreline erosion trends, numerical modeling of storm conditions with return periods of 10, 25, 50 and 100 years, and modeling of generalized storm conditions. These analyses provide the basis for the revetment damage progression analysis to estimate the useful life of the revetment. The analysis uses a probabilistic approach for the selection of storm events to calculate damage. An event is defined as offshore wave significant wave height ≥ 10 ft occurring for a minimum duration of 12 hours, using the record of waves at WIS Station ST82059. The results of the damage progression analysis indicate that the existing airstrip revetment will experience failure (exposure of the filter stone) in the next 10 – 15 years, assuming damage is solely caused by waves and maintenance and repair works are not performed on the revetment.

Alternatives are proposed to extend the life of the revetment and increase protection to the runway, including:

(1) Adding a layer of armor stone of the same class as the existing to the face of the revetment to increase the thickness of the revetment and thereby delay failure (exposure of the filter stone).

(2) Alternative (1) and raising the runway to minimize damage to the runway due to wave overtopping. The existing runway has an elevation of +16 ft NAVD88. The table below provides the required runway elevation, including a 1-ft freeboard, for the range of events and sea level projections considered in the study.

Table ES-.1 Required runway elevation including a 1-ft freeboard

SLR Projection (year)	SLR (ft)	Required Runway Elevation (ft, NAVD88)			
		10-yr	25-yr	50-yr	100-yr
2050	1.20	16	16	16	16
2060	1.89	16	16	16	16
2075	3.25	16	17	17.5	18
2100	6.32	19	20.5	21	21

(3) A third alternative involving new groins is discussed but it is not recommended at this time.

(4) No Action alternative. The analyses conducted in this report suggest that the size of the existing armor stone and overall design of the existing revetment are reasonable based on the storm conditions at Kivalina. Assuming the airport is relocated in 10 – 15 years, or the revetment is actively maintained, the No Action alternative is viable.

The proposed alternatives and No Action alternative should also consider performing maintenance and repair works in the summer months, paving the runway, and stabilizing the back slope on the lagoon side.

1.0 INTRODUCTION

Kivalina is a city located in northwestern Alaska, between Kotzebue Sound and Point Hope (Figure 1). The city sits at the southern end of a barrier island approximately 5.5 miles in length that separates the Kivalina Lagoon from the Chukchi Sea (Figure 1).

The coastline and infrastructure on the barrier island are vulnerable to damage by surge and waves associated with storms in the Chukchi Sea. The storms that cause the most damage tend to occur in the fall season prior to the formation of a consolidated sea ice cover. Once the sea ice and land-fast ice covers are established, the barrier island and the city are considerably less exposed to flood hazards. However, the scientific literature as well as accounts from residents suggest that global warming is already reducing the spatial and temporal coverage of sea ice in the Chukchi Sea, increasing the vulnerability of the barrier island to storms in the fall and early winter.

Damage from previous storms and observed and potential impacts of global warming have led the city to consider relocation from the barrier island to the mainland since 1994 (DOWL, 1994; USACE, 1998). In the interim, erosion control and shoreline protection works have been completed to protect the city. These include construction of two armor stone revetments: one around the south end of the barrier island completed in 2010 (USACE, 2020) and one along the seaward side of the airstrip completed in 2019. A causeway across the lagoon, connecting the city to the mainland, was built in 2021 to provide an evacuation route to residents in emergency situations arising from fall/winter storms.

The city has an airstrip that provides daily flights to Kotzebue, Alaska (Figure 2). The airstrip consists of a gravel runway, aligned parallel to the shoreline, approximately 3,000 ft in length and 60 ft in width. In the context of ongoing efforts to increase the resiliency of the city and ultimately relocate it, the Alaska Department of Transportation and Public Facilities (herein referred to as the DOT&PF) has tasked Stantec Consulting Services Inc. (Stantec) with: 1) estimating the remaining useful life of the existing airstrip revetment (completed in 2019) considering the extended exposure to storms in the fall/winter expected to occur due to global warming, 2) identifying alternatives to extend the useful life of the airstrip in its current location, and 3) provide cost estimates of those alternatives to compare against the cost of relocating the airstrip. This report presents the analyses carried out to address the first two objectives of the study.

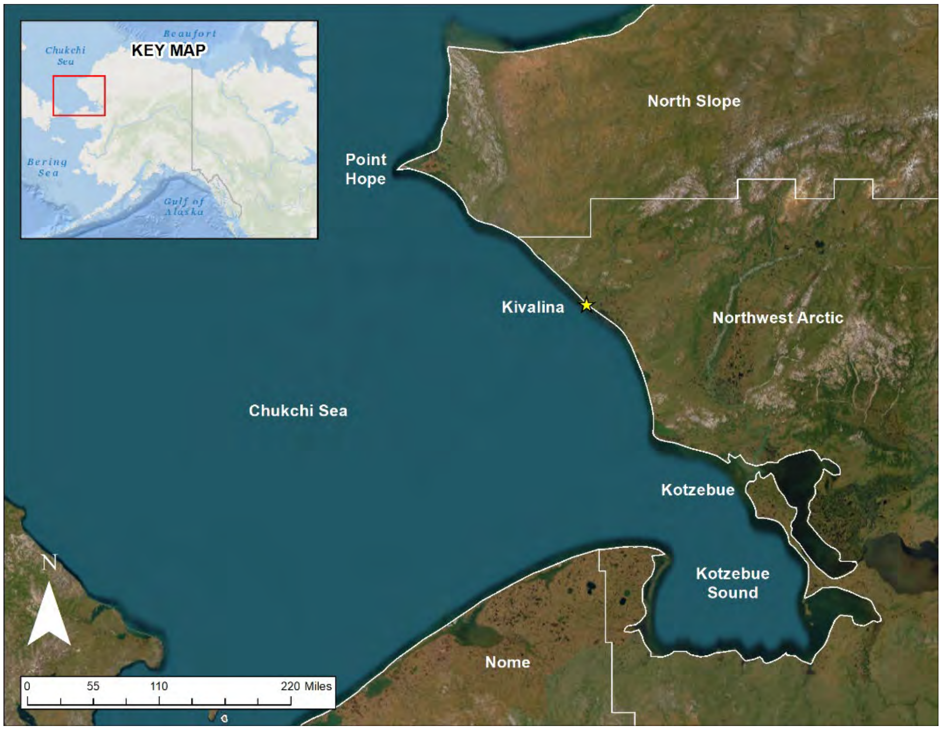

Figure 1. Location of Kivalina, Alaska

Figure 2. City of Kivalina, Alaska (Modified from USACE, 2016)

2.0 EXISTING AIRSTRIP REVETMENT

An armor stone revetment was constructed on the seaward side of the airstrip in 2019, as part of the Kivalina Airport Erosion Control project led by the DOT&PF, to protect the airstrip from erosion caused by storm events typical of the fall and winter. Figure 3 shows a photo of the revetment under construction.

Figure 3. Kivalina airstrip revetment under construction in 2019 (Brice Inc. website)

The Design Narrative Summary Memorandum by R&M Consultants (2018) provides the basis of design and recommended properties of the revetment. Table 1 provides a summary of the main design parameters. Figure 4 presents the “as-built” revetment cross-section, showing that the revetment includes a toe/launching section to provide stability and scour protection to the slope.

Table 1. Design parameters of existing airstrip revetment (R&M, 2018)

Design Parameter	Value	Design Parameter	Value
High Water (50-year SWL + wave setup) (ft, NAVD88)	+10.9	Armor Weight (lb)	2,000
Low Water (ft, NAVD88)	-3	Armor Thickness (ft)	4.6
Wave Height (ft)	6	Filter Weight (lb)	190
Wave Setup (ft)	1.3	Filter Thickness (ft)	2.4
Seaward Slope, α	1V:1.5H	Crest Elevation (ft, NAVD88)	15.0
Stability Coefficient, K_D	3.0	Armor Specific Gravity	2.65

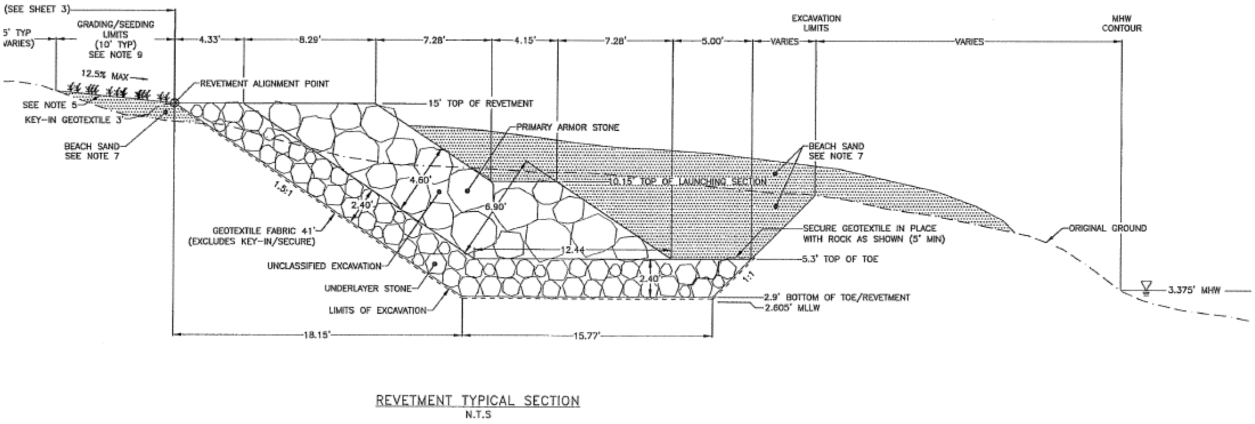

Figure 4. Kivalina airstrip revetment "as-built" cross section (DOT&PF, 2018)

The design filter and armor stone weights are assumed to follow Class II and Class IV riprap gradations, respectively, as specified in the DOT&PF Standard Specifications for Highway Construction (DOT&PF, 2020). These gradations are presented in Table 2.

Table 2. Riprap class of existing airstrip revetment layers

Revetment Layer	Class	Gradation (DOT&PF, 2020, Section 611)
Filter	Class II	50-100% weighing 200 pounds or more 0-15% weighing up to 25 pounds 0-10% weighing more than 400 pounds
Armor	Class IV	50-100% weighing 2,000 pounds or more 0-15% weighing up to 400 pounds 0-10% weighing more than 5,400 pounds

It is our understanding that the airstrip revetment has remained stable since its construction. The stability of the revetment can be attributed to its design armor stone weight, inclusion of a substantial toe, and proper construction. However, as mentioned in Section 1.0, a greater exposure to storm-driven waves in the fall and winter may pose a threat to the stability of the revetment, if not by a single storm, by the cumulative damage over the years. This report presents an analysis of such cumulative damage based on existing and future storm conditions. The basis of that analysis is founded on the analysis of meteorological and oceanographic (metocean) data, which is the subject of Section 3.0.

3.0 METOCEAN DATA ANALYSIS

Metocean data are analyzed to understand the conditions affecting the project site and inform the numerical modeling task described in Section 5.0. The metocean data analyzed include water levels, winds, and offshore waves. The location of the data points is shown in Figure 5.

Figure 5. Location of metocean data points

3.1 WATER LEVELS

The National Oceanic and Atmospheric Administration (NOAA) provide measurements of water levels at Station 9491094 Red Dog Dock, Alaska, located approximately 17 coast miles southeast from Kivalina. Given the proximity of the NOAA station to Kivalina, it is assumed that the data is representative of conditions at Kivalina.

3.1.1 Tide and Datums

The tide in the southern Chukchi Sea is of mixed, mainly semidiurnal type (Huang et al., 2012) which is characterized by two high and two low tides of unequal size every lunar day. Table 3 presents the tidal datums at Red Dog Dock provided by NOAA. The mean range of tide (MHW – MLW) is 0.71 ft.

Table 3. Tidal datums at NOAA Station 9491094 Red Dog Dock

Datum	Description	Elevation (ft, MSL)
MHHW	Mean Higher-High Water	0.51
MHW	Mean High Water	0.37
MSL	Mean Sea Level	0.00
MLW	Mean Low Water	-0.34
MLLW	Mean Lower Low Water	-0.49

From the “as-built” airstrip revetment drawings, which show MHW and MLLW relative to the North American Vertical Datum of 1988 (NAVD88), it is determined that MSL is 3 ft above NAVD88. This relationship was confirmed using the Alaska Tidal Datum Portal at Kivalina.

3.1.2 Storm Surge

Storm surge refers to the increase in water levels (above the predicted tide) caused by storms. Along the Chukchi Sea coastline, storm surge is most notably generated by extratropical, low-pressure centers (hereinafter referred to simply as storms) originating in the far north Pacific Ocean/Bering Sea and traveling northward towards the Bering Strait.

The time series of measured water levels (6-minute sample) at Red Dog Dock, shown in Figure 6, provides an indication of the magnitude of storm surge in the area. The top ten water level peaks within the available record are presented in Table 4. The storm surge estimated for each peak is calculated by subtracting the predicted (tidal) water level from the measured water level, both provided by NOAA at Red Dog Dock. Storm surge is observed to range from 4.5 to 7.4 ft.

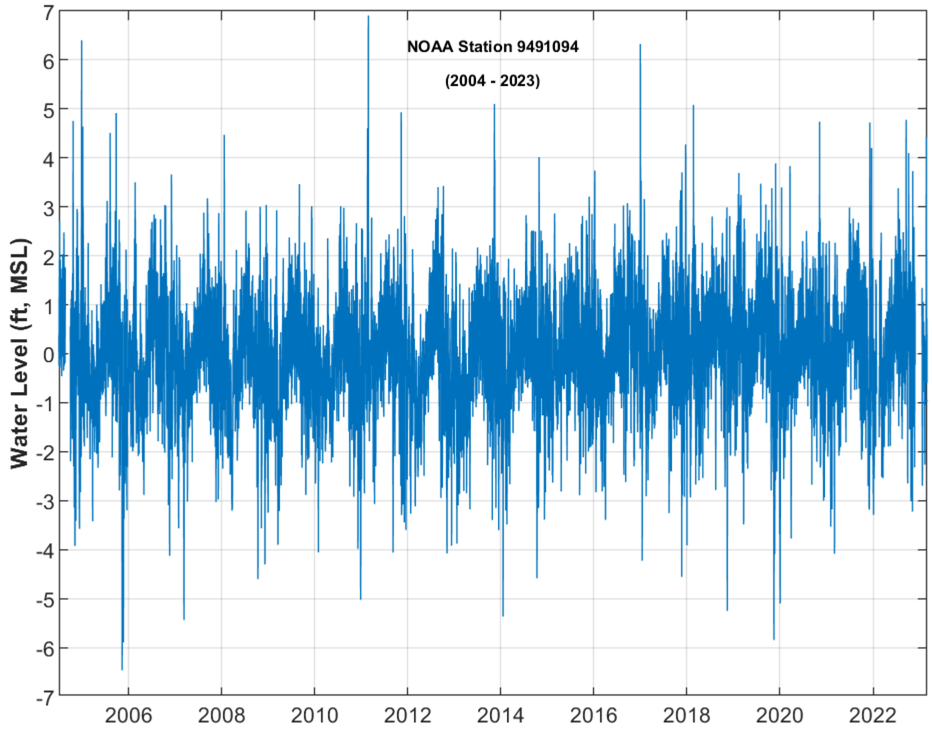

Figure 6. Measured water level at Red Dog Dock (2004 – 2023)

Table 4. Top ten measured water levels at Red Dog Dock (2004 – 2023)

Rank	Time of Peak (LST)	Measured Water Level (ft, MSL)	Predicted Water Level (ft, MSL)	Storm Surge (ft)
1	24-Feb-2011 21:36:00	6.91	-0.47	7.38
2	26-Dec-2004 00:36:00	6.40	0.14	6.26
3	30-Dec-2016 17:48:00	6.33	-0.18	6.51
4	10-Nov-2013 18:42:00	5.10	0.09	5.00
5	20-Feb-2018 16:06:00	5.09	-0.09	5.18
6	10-Nov-2011 00:42:00	4.93	0.18	4.75
7	23-Sep-2005 18:42:00	4.92	0.33	4.59
8	23-Sep-2005 23:54:00	4.79	0.15	4.64
9	18-Sep-2022 04:36:00	4.78	0.47	4.31
10	20-Oct-2004 03:48:00	4.75	0.22	4.53

The ten peaks presented in Table 4 occurred in the fall or winter. To further examine this seasonality, Table 5 presents the percent occurrence per month of events with water levels equal to or greater than 4 ft (MSL) for a total of 100 events. The analysis indicates that, indeed, high water levels (driven by storm surge) tend to occur in the months of September through February (i.e., fall and winter seasons). This is an important observation in the context of global warming effects on the formation of the sea ice cover in the Chukchi Sea. It suggests that, as the sea ice cover reduces in time and space in the fall and winter, Kivalina will be at an even greater risk of incurring storm-related damage.

Table 5. Occurrence per month of water levels ≥ 4 ft (MSL) at Red Dog Dock (2004 – 2023)

Month	Percent Occurrence	Month	Percent Occurrence
January	15	July	0
February	8	August	1
March	0	September	20
April	0	October	17
May	0	November	22
June	0	December	17

The storm tracks associated with peaks 7 and 8 (September 2005) and peak 10 (October 2004) in Table 4 are available from Pingree-Shippee et al. (2016) and presented here as Figure 7. These are presented to illustrate storm tracks that have resulted in high storm surge at the coast in the vicinity of Kivalina. These storm tracks fall into one of three well-known general storm tracks in the Bering and Chukchi Seas, which are characterized by storms traveling northward through the central Bering Sea (Pingree et al., 2016). It is reasonable that storms traveling in this general track will generate storm surge at the northwest coast of Alaska, due to the counterclockwise cyclonic winds pushing water towards the right front quadrant of the storm.

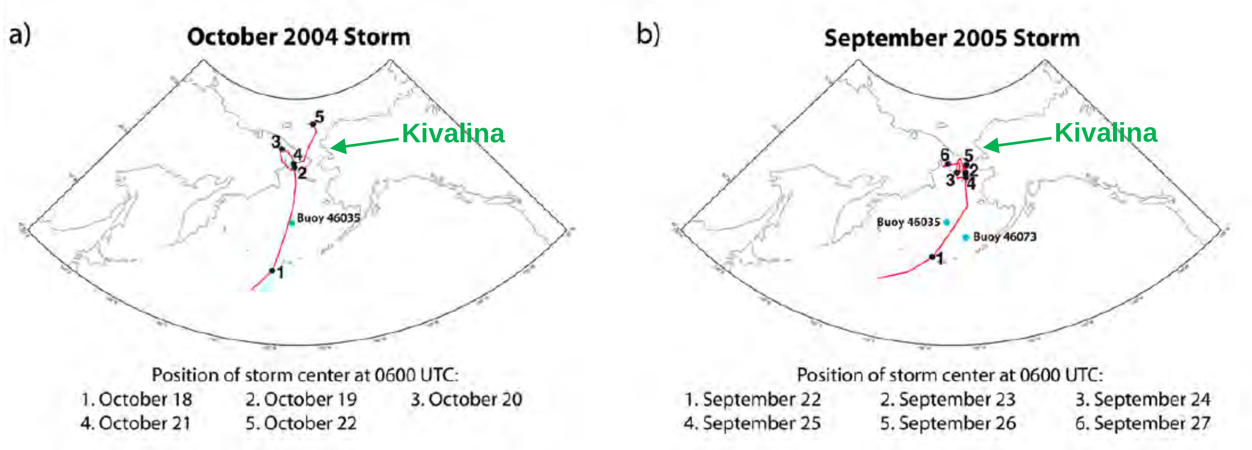

Figure 7. October 2004 and September 2005 storm tracks (Pingree-Shippee et al., 2016)

Measured water levels are useful in understanding storm surge along a coastline. However, they are limited to the record of measurements and the storms that have occurred during that time. Estimates of probabilistic storm surge at a site for design of coastal structures are commonly developed by modeling many (up to hundreds) of storms to capture the variability of storm tracks and storm parameters. Table 6 provides estimates of storm surge at Kivalina for a range of return periods obtained from USACE (2016). These were used as part of the basis of design for the causeway across Kivalina Lagoon that was completed in 2021 and are used in this study as the basis for extreme water levels.

Table 6. Probabilistic storm surge at Kivalina (USACE, 2016)

Return Period (years)	Annual Exceedance Probability	Storm Surge (ft)	Peak Water Level (ft, MSL)
5	0.20	3.5	3.9
10	0.10	4.3	4.7
20	0.05	5.4	5.8
25	0.04	5.6	6.0
50	0.02	6.2	6.6
100	0.01	6.4	6.8

3.2 WINDS

Winds measured at Kivalina Airport (METAR PAVL) from August 1998 to October 2022 are analyzed to characterize the wind conditions. Wind speeds are assumed to be 2-minute average values at a height of 33 ft which is the standard format for an Automated Surface Observation System (ASOS) (NOAA, 1998).

Figure 8 shows seasonal wind roses developed from the record of winds. Two primary wind conditions are discernable: dominant winds from the N – NE – E sector in the fall, winter, and spring, and dominant winds from the SSE – S – SSW and W – WNW sectors in the summer. Wind speeds are statistically the lowest in the summer and the highest during the winter. The seasonality is primarily dictated by the dynamics of the Aleutian Low-Pressure System and its interaction with arctic and continental air masses (Overland, 1981; Stabeno et al., 1999).

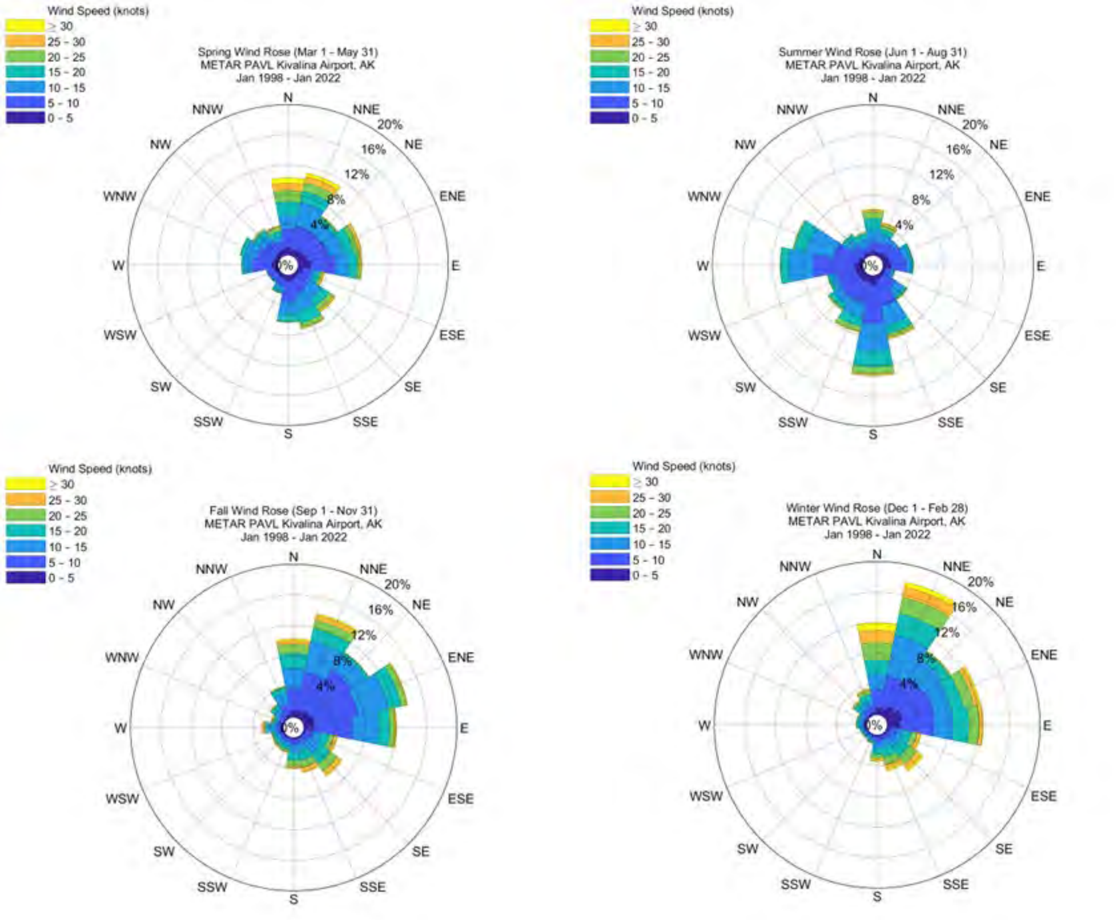

Figure 8. Seasonal wind rose from wind record at Kivalina Airport: Spring (top left), Summer (top right), Fall (bottom left), Winter (bottom right)

Approximately 60 – 65% of the winds in the fall and winter come from the N – E sector. The barrier island that is home to Kivalina has a NW – SE alignment. Therefore, winds from the N – E sector are generally not driving waves towards the coastline.

3.3 OFFSHORE WAVES

The Wave Information Studies (WIS) is a coastal wave hindcast model developed by the U.S. Army Corps of Engineers (USACE) that provides offshore winds and waves at points along the U.S. coast, including northwestern Alaska. The closest WIS station to Kivalina is ST82059, located approximately 16 miles from the coastline in 28 m (92 ft) water depth (Figure 5).

A characterization of offshore wave conditions is presented based on analysis of the WIS data for present and future sea ice conditions.

3.3.1 Present Sea Ice Conditions

In areas where sea ice forms in the winter and affects wave growth and propagation, such as the Chukchi Sea, the WIS transforms a grid point from active to inactive (water to land) when the ice concentration is 70% or greater (personal communication, April 2023). For this reason, the time series of significant wave height and peak wave period at ST82059, shown in Figure 9, have gaps in the winter and spring months.

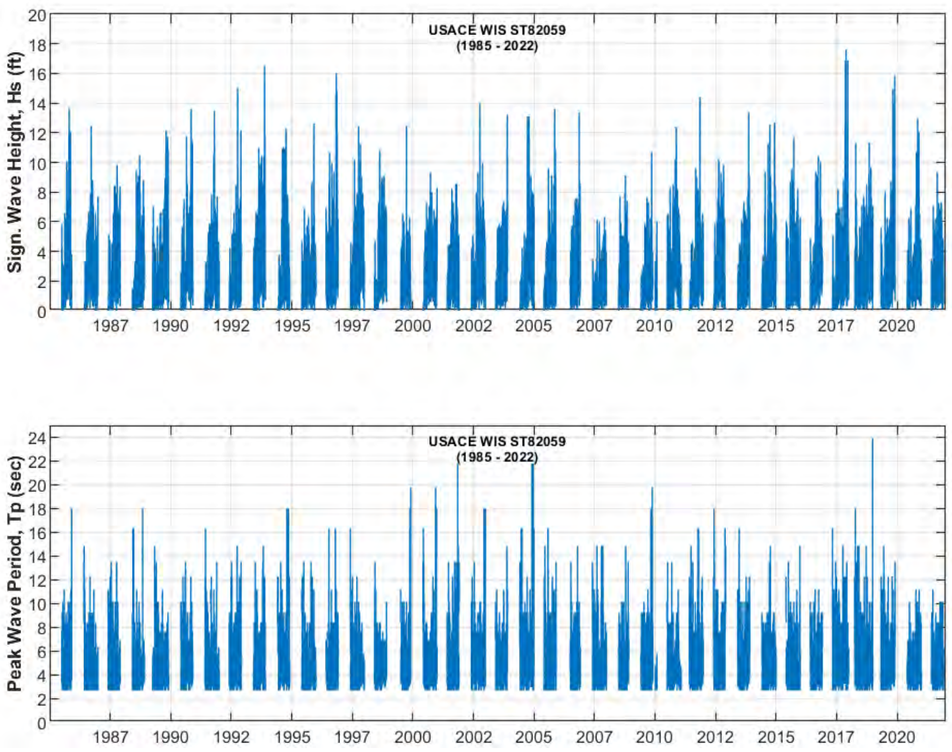

Figure 9. Time series of significant wave height and peak wave period at WIS ST82059

Figure 10 presents the annual significant wave height and peak wave period roses developed from the available data, showing the directional distribution of offshore wave heights and wave periods. The roses are presented for the summer and fall seasons only, as the winter and spring seasons have significant gaps due to the sea ice cover.

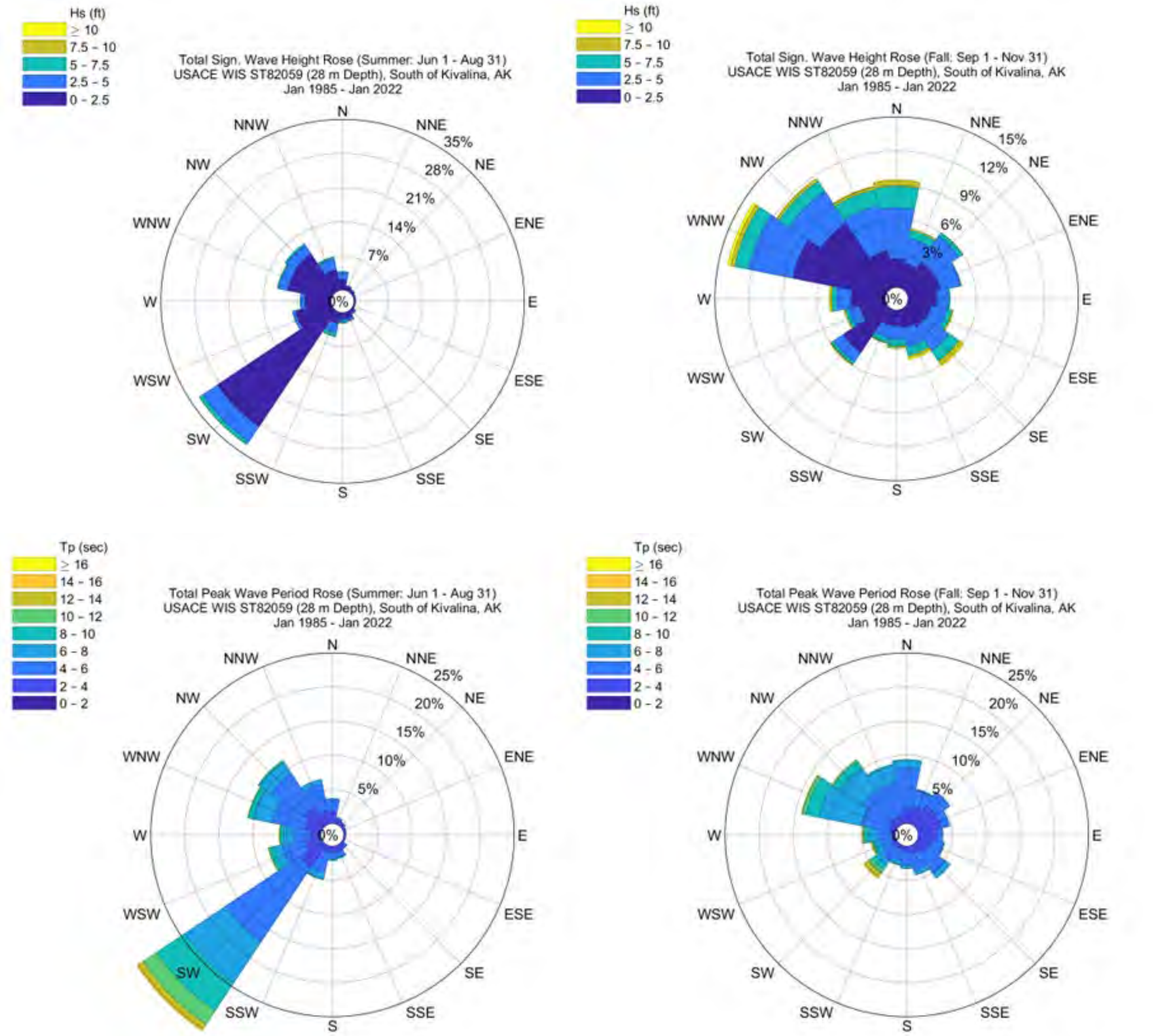

Total Sign. Wave Height Rose (Summer: Jun 1 - Aug 31)
USACE WIS ST82059 (28 m Depth), South of Kivalina, AK
Jan 1985 - Jan 2022

Total Sign. Wave Height Rose (Fall: Sep 1 - Nov 31)
USACE WIS ST82059 (28 m Depth), South of Kivalina, AK
Jan 1985 - Jan 2022

Total Peak Wave Period Rose (Summer: Jun 1 - Aug 31)
USACE WIS ST82059 (28 m Depth), South of Kivalina, AK
Jan 1985 - Jan 2022

Total Peak Wave Period Rose (Fall: Sep 1 - Nov 31)
USACE WIS ST82059 (28 m Depth), South of Kivalina, AK
Jan 1985 - Jan 2022

Figure 10. WIS ST82059 wave roses for summer (left) and fall (right)

There is an appreciable distinction between summer and fall offshore wave conditions, which is described as follows:

- Summer wave conditions are characterized by low wave heights, with the following frequency of occurrence: Hs ≤ 2.5 ft about 73%, 2.5 ft < Hs ≤ 5 ft about 17%, and Hs > 5 ft about 3.5%. Waves approach from the western half of the compass, with waves from the SW accounting for approximately 45% of the waves. Waves from the SW have longer wave periods in general, including a small percentage of waves (about 3.5%) with Tp > 12 seconds. The Bering Strait is precisely located to the SW of ST82059, suggesting that wave conditions in the summer can be influenced by swell from the Pacific Ocean.
- Fall wave conditions are characterized by higher wave heights, compared to the summer, with the following frequency of occurrence: Hs ≤ 2.5 ft about 50%, 2.5 ft < Hs ≤ 5 ft about 35%, and Hs > 5 ft about 15%. Peak wave periods are predominantly below 8 sec, exceeding 10 sec about 5 % of the time. Waves approaching from the WNW – NW – N sector occur most frequently, accounting for about 45% of the waves.

3.3.1.1 Storm Waves

As discussed in Section 3.1.2, storms originating in the north Pacific Ocean and Bering Sea, some of which enter the Chukchi Sea, occur in the fall and winter months. Without a historical record of storm tracks for this region, an approach to identify and examine the characteristic of storm waves from the WIS record is by establishing a wave height threshold.

The WIS provides an extreme value analysis of the significant wave height at ST82059 using a peak-over-threshold approach with a threshold of Hs > 6.3 ft (calculated as the mean value plus one standard deviation). The frequency curve from the extreme value analysis by WIS is shown in Figure 11. The plot also provides the linear fit equation to predict the significant wave height for a given return period and the top 10 events based on the prescribed threshold.

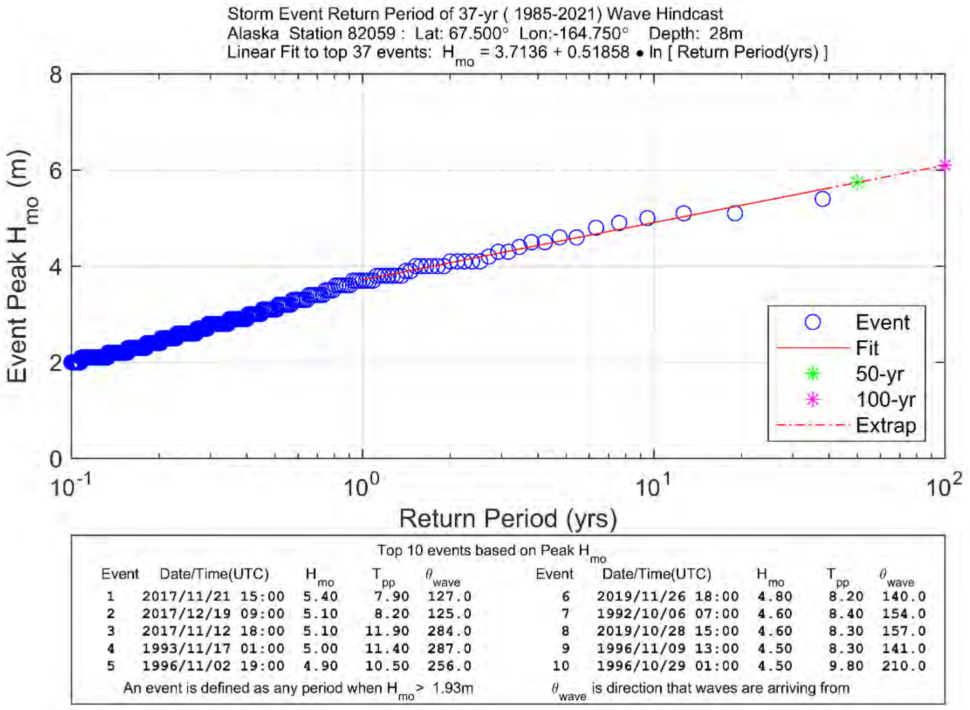

Top 10 events based on Peak H_{mo}

Event	Date/Time(UTC)	H_{mo}	T_{pp}	θ_{wave}	Event	Date/Time(UTC)	H_{mo}	T_{pp}	θ_{wave}
1	2017/11/21 15:00	5.40	7.90	127.0	6	2019/11/26 18:00	4.80	8.20	140.0
2	2017/12/19 09:00	5.10	8.20	125.0	7	1992/10/06 07:00	4.60	8.40	154.0
3	2017/11/12 18:00	5.10	11.90	284.0	8	2019/10/28 15:00	4.60	8.30	157.0
4	1993/11/17 01:00	5.00	11.40	287.0	9	1996/11/09 13:00	4.50	8.30	141.0
5	1996/11/02 19:00	4.90	10.50	256.0	10	1996/10/29 01:00	4.50	9.80	210.0

An event is defined as any period when H_{mo} > 1.93m

θ_{wave} is direction that waves are arriving from

Figure 11. WIS ST82059 extreme value analysis (provided by WIS)

To examine the characteristics of storm waves, wave roses are developed for the threshold of Hs > 6.3 ft from WIS and for three additional thresholds: 7.5 ft, 10 ft, and 12.5 ft. The wave roses are presented in Figure 12 and the respective wind roses in Figure 13.

Examination of the roses suggests that as the threshold wave height increases, the prevailing direction of wave approach is the SE and WNW, which corresponds to the sectors with the longest fetch (Figure 14). The fetch from the SE is provided by Kotzebue Sound, while the fetch from the WNW is bounded by the Siberian coast of Russia. In addition, the roses show that wind and wave directions are well correlated, especially as the threshold wave height increases, suggesting that storm waves are generated by winds within the Chukchi Sea.

Winds and waves may come from both SE and WNW during the same storm, as exemplified by the November 2017 storm whose time series of wind and wave directions is shown in Figure 21. In the case of this storm and many others in the WIS record, winds initially approach from the SE sector and shift clockwise to the northwestern sector, driving waves towards the coastline in the same fashion.

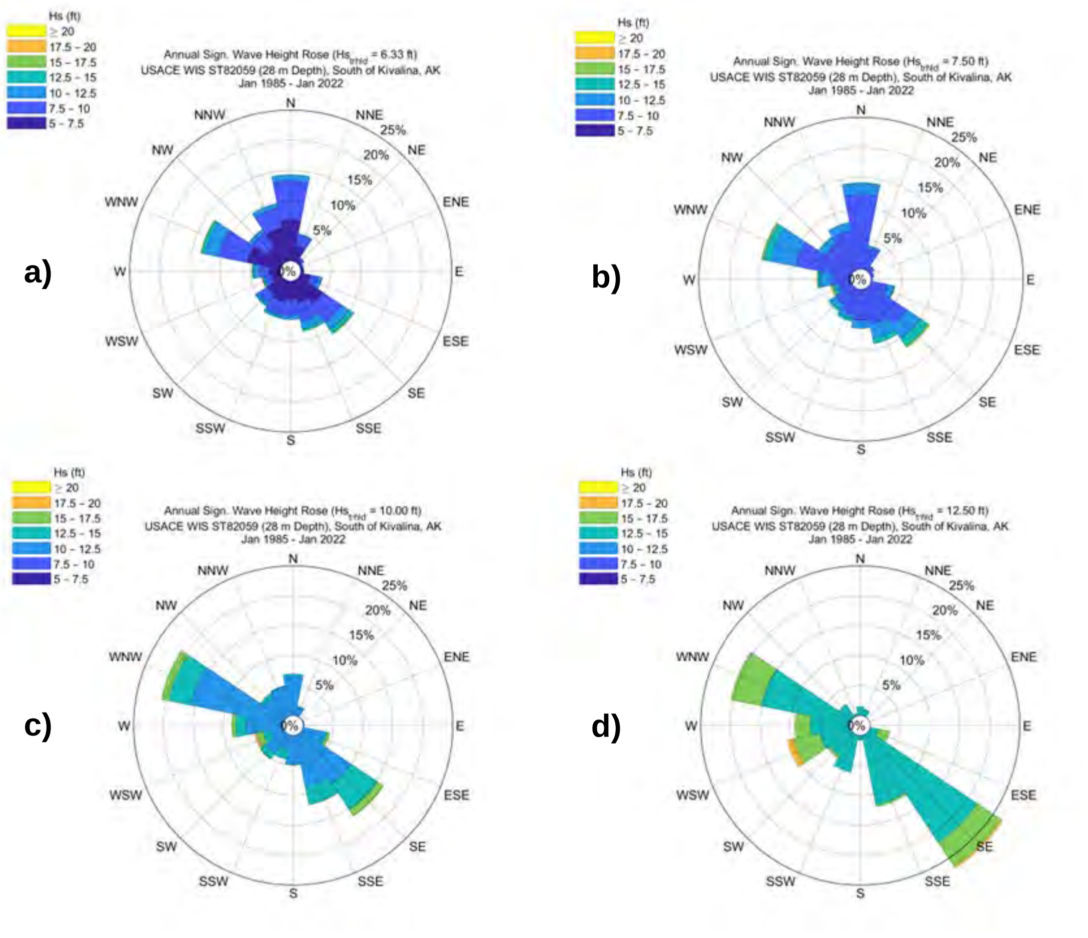

Figure 12. WIS ST82059 significant wave height roses for a range of thresholds: a) Hs > 6.3 ft, b) Hs > 7.5 ft, c) Hs > 10 ft, and d) Hs > 12.5 ft

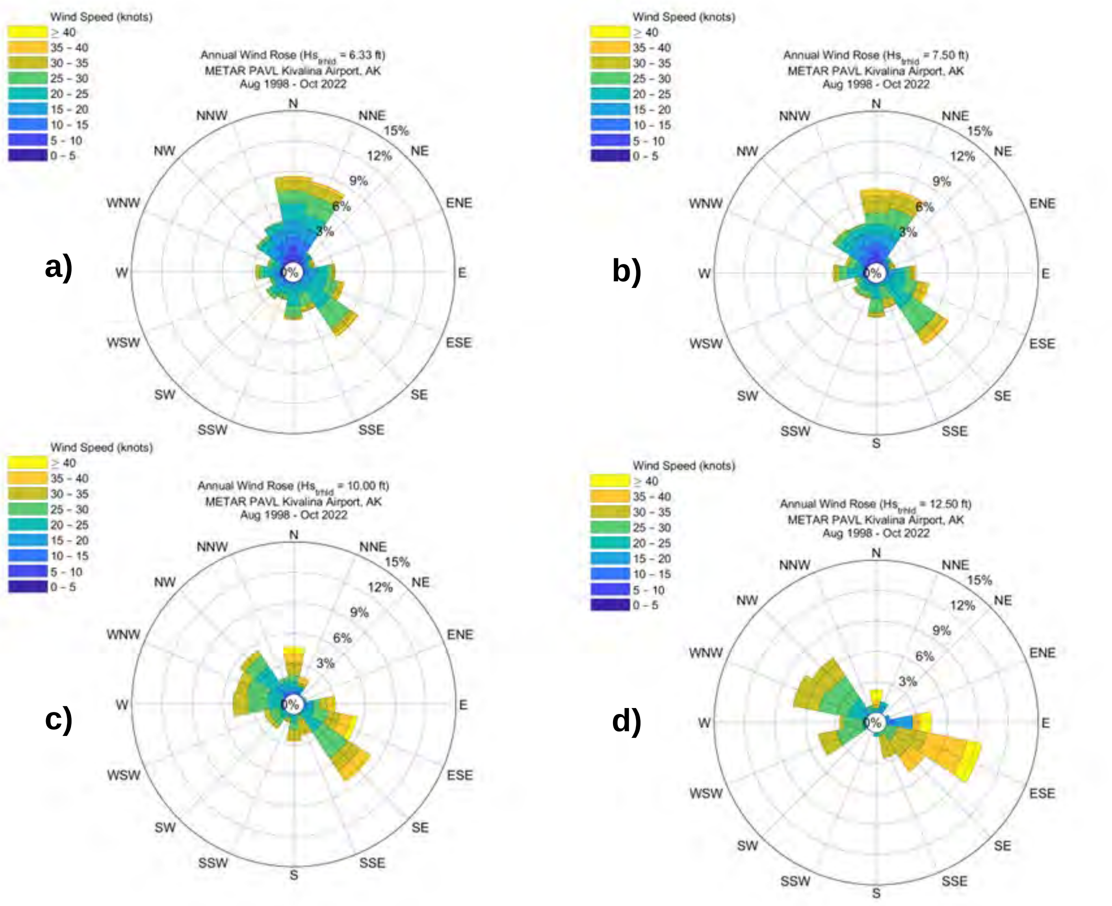

Figure 13. WIS ST82059 wind roses for a range of thresholds: a) Hs > 6.3 ft, b) Hs > 7.5 ft, c) Hs > 10 ft, and d) Hs > 12.5 ft

Figure 14. Fetch to the SE and WNW at WIS ST82059, including significant wave height rose for Hs > 12.5 ft

3.3.2 Future Sea Ice Conditions

Fang et al. (2018) analyzed sea ice concentration data relevant to Kivalina and observed that, due to global warming, “the open-water season has increased by 5.6 ± 1.2 days/decade over the last 37 years, with moderate evidence that it is extending further into the fall than into the spring.”

The offshore wave and wind data from WIS ST82059 is nonexistent in the winter and spring months due to the presence of sea ice. In a future where global warming continues to reduce the spatial and temporal coverage of sea ice in the Chukchi Sea, wave dampening by the sea ice will lessen and potentially cease to exist. With sea ice reduction, the Kivalina coastline will become increasingly exposed to waves and particularly to storm waves that occur in the Chukchi Sea in the winter months (refer to Table 5).

Prediction of offshore waves to fill in the gaps in the WIS data is carried out using a machine learning algorithm. The approach consists of using the wind speeds measured at the Kivalina Airport and the WIS wave height and period to train an algorithm to predict wave height and period based on wind speed. The record of winds from the Kivalina Airport begins in 1998 and, therefore, the prediction of offshore waves is restricted to the period 1998 – 2022. Figure 15 shows the time series of significant wave height and peak wave period resulting from the machine learning algorithm. The mean square error is 0.03 ft and 0.2 sec for significant wave height and peak wave period, respectively.

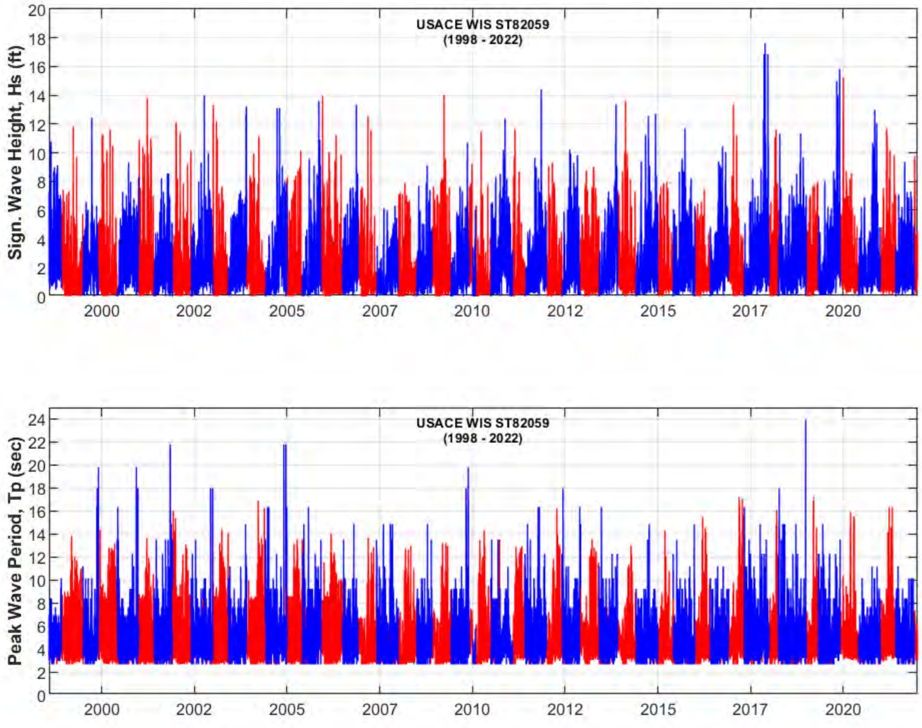

Figure 15. Predicted wave parameters (red line) for WIS ST82059

The main limitation with the methodology used to predict offshore waves is that the algorithm does not incorporate wind direction. Stantec found that the correlation between wind direction from WIS and airport is poor overall. This limitation, however, builds conservatism in the use of the predicted wave heights in the damage progression analysis.

3.4 RELATIVE SEA LEVEL CHANGE

Relative sea level (RSL) change is the change in mean sea level resulting from global phenomena associated with warming of the oceans and melting of polar ice as well as local ground surface vertical movement. Relative sea level change may be positive (rising) or negative (falling), depending on site specific conditions. Figure 16 presents an illustration of relative sea level change and scenarios that result in positive or negative RSL change.

According to estimates in DeGrandpre (2015), Kivalina is experiencing positive RSL change of 0.69 mm/year, with -0.31 mm/year of mean sea level change and -1.0 mm/year of land movement. The positive RSL results because the land is subsiding faster than the rate at which mean sea level change is falling (Figure 16). DeGrandpre (2015) suggests that this regime applies to most of Northwestern Alaska.

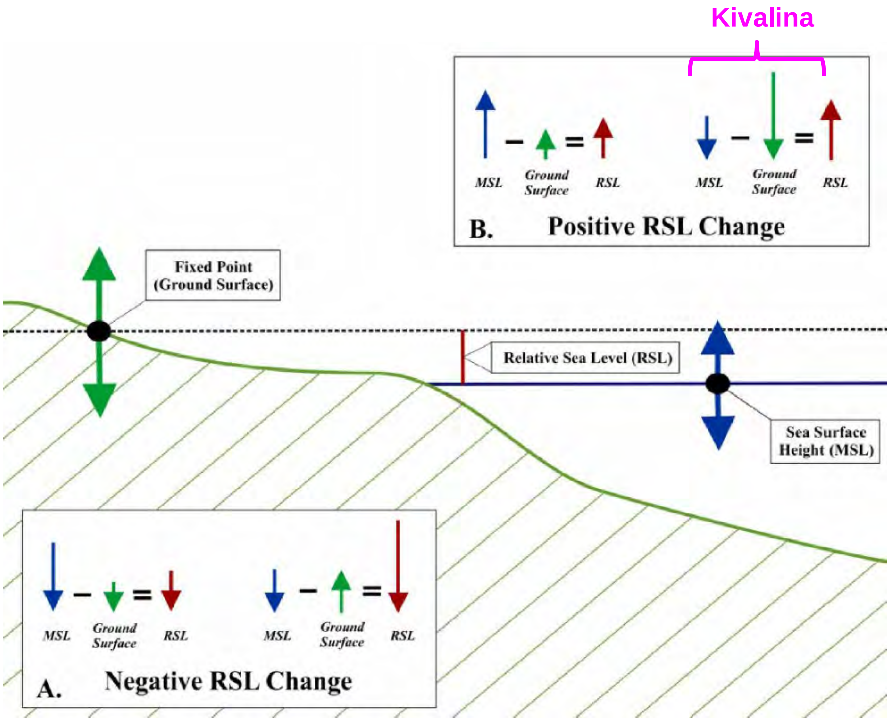

Figure 16. Relative sea level change diagram (Adapted from DeGrandpre, 2015)

A RSL change projection is necessary to plan and design accordingly. The RSL projections for Nome, Alaska, based on Sweet et al. (2017) and available through the online NOAA Sea Level Change Calculator are the closest to Kivalina. According to DeGrandpre (2015), Nome experiences a RSL change of 0.85 mm/year, which is higher than at Kivalina. Therefore, the use of RSL projections for Nome for Kivalina can be considered conservative. The projections for years 2050, 2060, 2075 and 2100 are summarized in Table 7 with respect to year 2023.

Table 7. Relative sea level change projections assumed for Kivalina (in feet)

Year (w.r.t 2023)	Low	Intermediate - Low	Intermediate	Intermediate - High	High
2050	0.18	0.21	0.49	0.76	1.20
2060	0.21	0.28	0.75	1.22	1.89
2075	0.29	0.44	1.22	2.12	3.25
2100	0.41	0.67	2.22	4.11	6.32

4.0 SHORELINE DYNAMICS

In the coastal region, sediment transport is most active in the surf zone (zone of wave breaking) because of the combination of high turbulence associated with wave breaking and shallow water, which agitates and sets sediment particles in motion. Sediment transport in the surf zone has a longshore and cross-shore component. These are described below in the context of the summer and fall seasons during which sea ice in the nearshore of Kivalina is absent. Sediment transport significantly reduces once the sea ice and land fast ice cover are established in the winter and through the spring.

Longshore sediment transport is driven by shore-parallel currents generated by waves breaking at an angle to the coastline. The prevailing longshore sediment transport along the Kivalina coastline is northward (USACE, 2007). This is consistent with the prevailing waves from the southwest during the ice-free season when sediment transport is active. However, as discussed in Section 3.3, waves associated with storms in the fall/winter have a strong northwesterly component, which causes significant longshore sediment transport southward.

Cross-shore sediment transport occurs perpendicular to the shoreline, either seaward or shoreward, primarily due to wave orbital velocities and undertow (Tajima and Madsen, 2005). Low-energy wave conditions tend to yield net shoreward sediment transport that nourishes the beach, while high-energy wave conditions result in net seaward sediment transport that creates nearshore bars (Figure 17). In Kivalina, low-energy wave conditions prevail in the summer, allowing the shoreline to be nourished, whereas high-wave energy conditions and the passage of storms in the fall move sediments to the offshore bars, resulting in shoreline retreat.

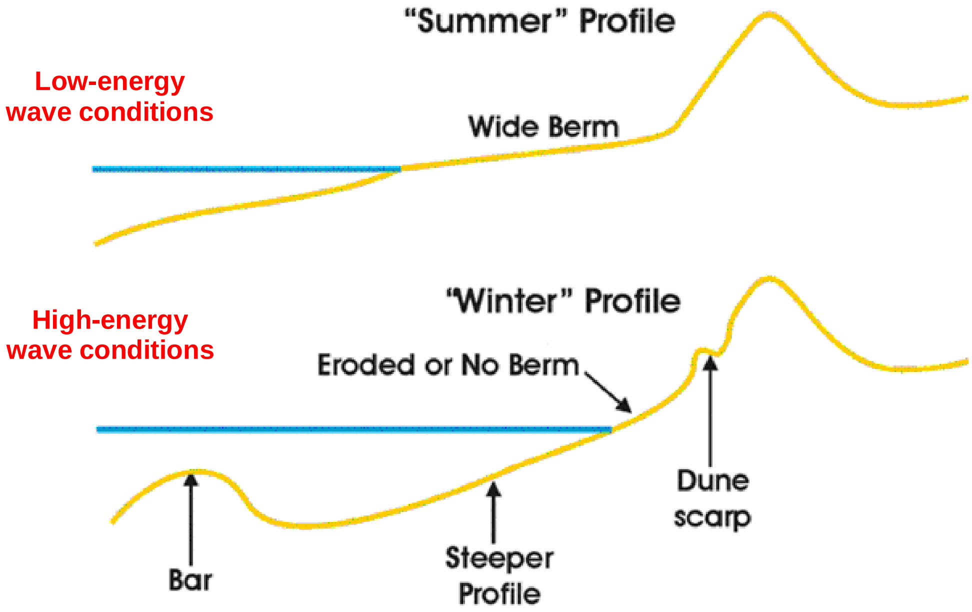

Figure 17. Illustration of cross-shore sediment transport on beach profile

The Kivalina shoreline is primarily composed of medium sand. Sandy gravel from the Wulik and Kivalina rivers is also present, primarily near the inlets (DOT&PF, 1984). Shoreline dynamics on the seaward side of the barrier island has been studied previously. The following are excerpts from studies that describe episodic erosion and long-term sediment dynamics in the Kivalina shoreline.

- DOWL (1994). “Review of photographs, back to 1952, does not show conclusive proof that erosion is occurring on the Chukchi Sea side of the island. The beach and the southeast end of the island at the Singalliik Entrance are such dynamic systems that at times it is eroding and, at other times, it is adding.”
- NOAA (2004). “The erosion accretion pattern observed here may indicate that this portion of coast is in the process of normal erosion associated with offshore transport of materials with a net loss of area due to erosion. This may or may not be considered significant erosion from 1952 to 2003.”
- USACE (2006). “Kivalina has not historically seen significant erosion. The Kivalina spit has seen cyclic erosion and accretion, with modest accretion on the Chukchi Sea side more prevalent during the 30-year period of 1970 to 2000.”
- USACE (2007)
    - “Storm events in 2004 and 2005 caused 25 to 30 feet of beach erosion along the shoreline and 20 feet of beach erosion towards the airstrip. Storms in September and October 2006 resulted in erosion up to 50 feet inland and exposed the permafrost in some areas.”
    - “Although the coastal water mass flows northward at a fairly steady rate, the net longshore drift of gravel on the beach at Kivalina is southward because of large storms from the northwest that overpowers the surface flow and directs it southward along the beach.”
- HDR (2016). “In October 2015, a storm caused substantial erosion to the coastline (approximately 10 feet in one day) near the runway.”
- R&M (2018)
    - “The overall erosion and accretion appear to generally be in balance over the past 30 years or more.”
    - “The erosion pockets have normally shoaled back in within one or two seasons only to reoccur at different locations. Although the long-term erosion appears to be in a state of near equilibrium, extreme storm events will continue to occur and the runway will continue to be threatened without coastal protection.”

In summary, this non-exhaustive list of studies suggests that 1) significant shoreline erosion has occurred during storm events and 2) there is no definitive long-term shoreline erosion trend.

The latter observation is also supported by the historical and future shoreline positioning from the Alaska Shoreline Change Tool (DGGS, 2015) along the Kivalina airstrip. Figure 18 shows shoreline retreat between 1952 and 1980, shoreline advance between 1980 and 2003, and practically stable conditions between 2003 and 2013. In addition, projections for 2025 and 2030 show a stable shoreline that is >100 ft from the airstrip. The horizontal extent of the existing revetment is approximately 35 ft from the seaward edge of the airstrip.

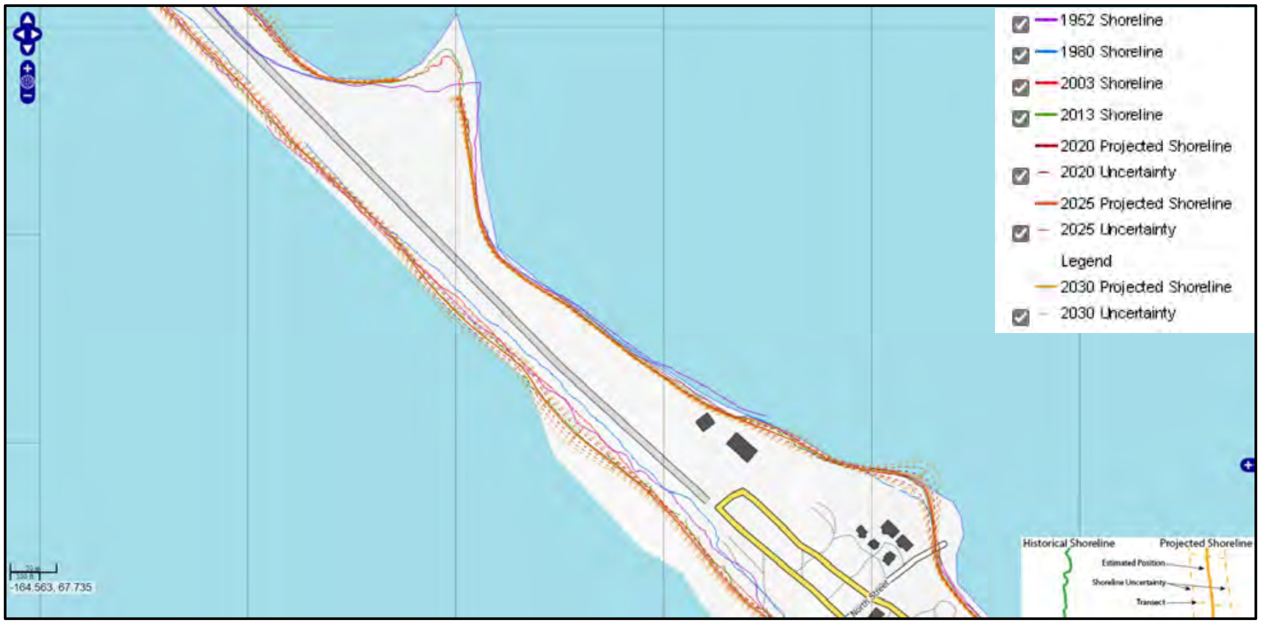

Figure 18. Shoreline position along Kivalina airstrip from Alaska Shoreline Change Tool

As the sea ice cover reduces due to global warming, the Kivalina shoreline will be increasingly exposed to storms that can cause shoreline retreat. The absence of a sea ice cover is not captured in the studies listed above or predictions from the Alaska Shoreline Change Tool, which are primarily based on aerial images and anecdotes. It can also be argued, however, that the period of relatively calm wave conditions will lengthen without the sea ice cover (for example, during the ice-free spring season), providing more time for transport of sediment from the offshore bars to the beach. A key factor is whether the frequency of storms will increase due to global warming, relative to present conditions, and if the increase will be such that the beach recovery time will not be sufficient to counteract erosion and maintain a relatively stable shoreline.

The Kivalina airstrip revetment provides the last line of defense to the runway against erosion. The revetment was constructed with a substantial toe/launching section designed to fill in areas of scour that develop at the base to continue to provide support to the armor stone on the slope. Based on the apparent stability of the shoreline and considering the inclusion of a toe in the design of the revetment, it is reasonable to assume that damage to the revetment by waves is more likely and destructive than that from short- or long-term erosion. Therefore, this study estimates the useful life of the revetment based only on wave-induced damage, as discussed in Section 6.2, without the need for shoreline evolution modeling. Nonetheless, there are solutions to enhance the stability of the shoreline to combat the increased exposure to storms if climate change continues to reduce the sea ice cover in the Chukchi Sea. These solutions are discussed in Section 7.0.

5.0 MODELING OF STORM CONDITIONS

Numerical modeling of storm conditions was carried out to estimate water level and wave parameters in the proximity of the existing airstrip revetment for input to the damage progression analysis (Section 6.2) and generate inundation maps of the barrier island.

5.1 SOFTWARE

The MIKE 21 Hydrodynamic and Spectra Wave modules (herein referred to as HD and SW modules) were used to simulate storm surge and wave propagation, respectively, from offshore to the barrier island. The following are short descriptions of the MIKE 21 modules:

- The HD Module simulates unsteady flow considering density variations, bathymetry, and external forcings in coastal areas, estuaries, rivers, and lakes. The model solves the continuity, momentum, temperature, salinity, and density equations.

- The SW Module is a third-generation spectral wind-wave model that simulates the growth, decay, and transformation of wind-generated waves and swells in offshore and coastal areas. The model includes the following physical phenomena: wave growth by action of wind, non-linear wave-wave interaction, dissipation due to white-capping, dissipation due to bottom friction, dissipation due to breaking, refraction, and shoaling due to depth variation; and wave-current interaction.

5.2 MODEL DOMAIN

The model domain, shown in Figure 19**,** is based on the geographic extent of available data sources as well as the potential hydrodynamic influences from the boundaries. The offshore boundary is set at the location of the offshore wind and wave data available from WIS ST82059.

The sources of ground elevation data include NOAA Chart #16005, lagoon multi-beam transect surveys, and upland LiDAR Digital Terrain Model (DTM). These data were interpolated onto a computational mesh of triangular elements. The mesh was generated with horizontal mesh sizes varying from hundreds of meters to tens of meters, where finer resolution is used in the vicinity of project infrastructure and in areas required to represent the changes of nearshore bathymetry and shoreline topography. Figure 20 shows the mesh resolution in the vicinity of the Kivalina barrier island.

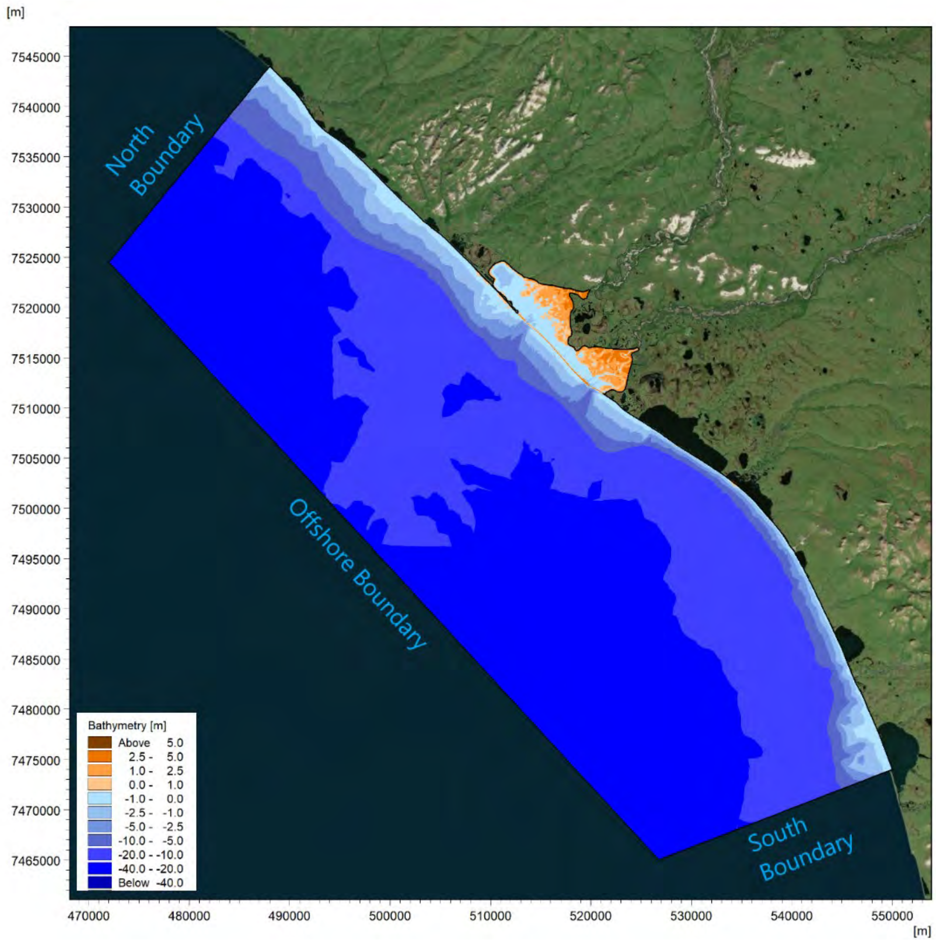

Figure 19. Computational domain and elevation contours

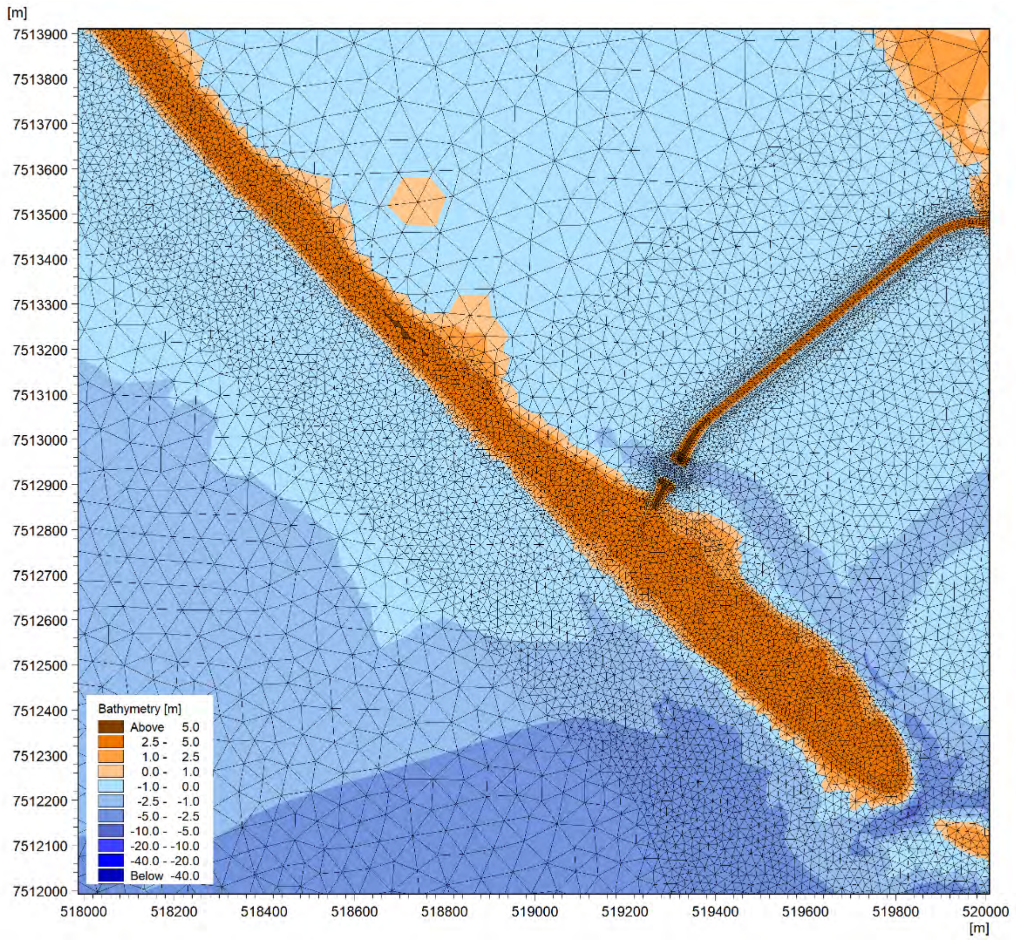

Figure 20. Mesh resolution and elevations in the vicinity of Kivalina

5.3 SIMULATIONS

Three sets of simulations are presented: Nearshore Waves: Extreme Events, Inundation Mapping: Extreme Events, and Generalized Storm Conditions.

5.3.1 Nearshore Waves: Extreme Events

The goal of these simulations is to determine the wave parameters associated with extreme events in the nearshore of Kivalina in present day and considering RSL change in 2050, 2075, and 2100. The nearshore wave parameters are then used to determine the hypothetical armor stone size of the airstrip revetment for comparison against the existing airstrip revetment (refer to Section 6.1).

The extreme events are the 10-, 25-, 50-, and 100-year events. The boundary conditions for the events are generated by scaling the time series of water level, offshore wave, and wind speed associated with the No. 1 event (based on peak wave height) in the WIS ST82059 record of November 21 – 25, 2017. The time series of this event is shown in Figure 21. This event was chosen for the following reasons:

- It is the No. 1 peak in the WIS ST82059 record when ranking the Hs from high to low. Wave parameters at the peak of the event are Hs = 17.7 ft, Tp = 7.9 sec.
- The event features two wave height peaks of nearly the same magnitude. The duration of the peaks is approximately two days.
- Offshore wave directions cover a wide sector, from 130 °N and clockwise to 300 °N, which suggests the storm traversed the Chukchi Sea from south to north. This is the most adverse track for the Northwestern Alaska shoreline, due to the counterclockwise rotation of winds in the northern hemisphere pushing storm surge and waves towards the coast.
- Water levels from Red Dog Dock are available for this period.
- Compared to the top 10 peaks in the WIS ST82059 record, this event is overall the most conservative event for the purposes of this study.

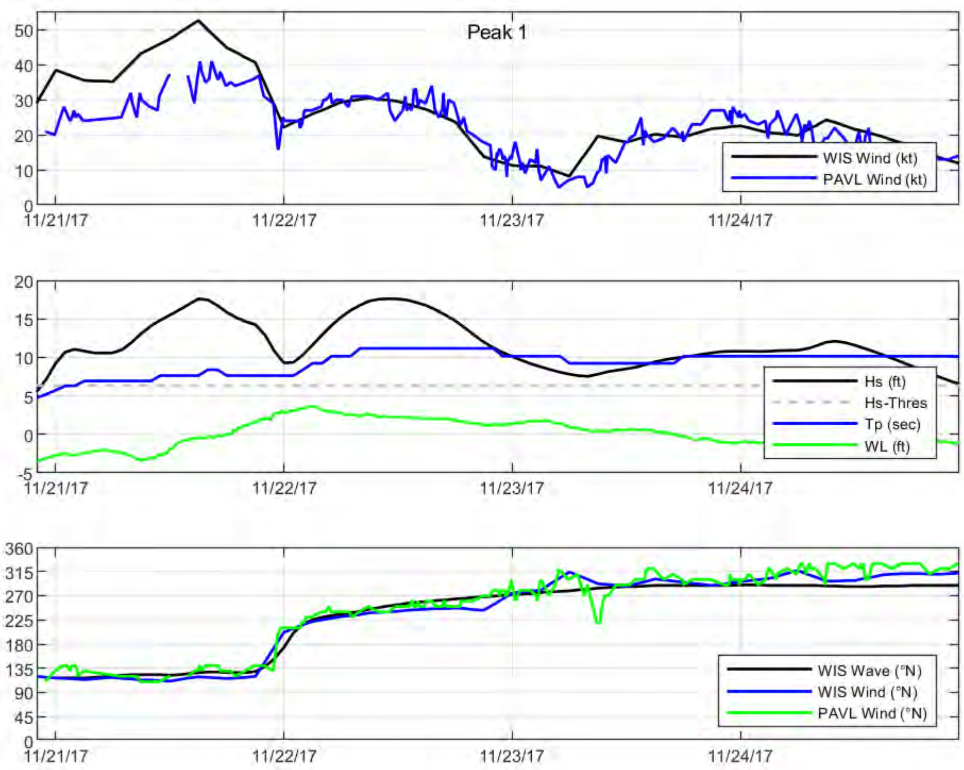

Figure 21. Event ranked no. 1 from WIS ST82059 record based on peak wave height

The time series of waves, winds, and water level of the selected event are processed as follows:

- Water levels are scaled using the extreme water levels from USACE (2016) (Table 6) such that the peak water level matches the desired return period.
- Offshore significant wave heights are scaled using the formulation provided in the extreme value analysis from WIS for ST82059 such that the peak wave height matches the desired return period. The same procedure is applied for the wind speed.
- Offshore peak wave periods are calculated assuming wave steepness (ratio of wave height to wavelength) is preserved with respect to the original event.
- Offshore wave direction and wind direction are the same for all return periods.

Figure 22 shows the time series of the events. Table 8 presents the maxima of each event.

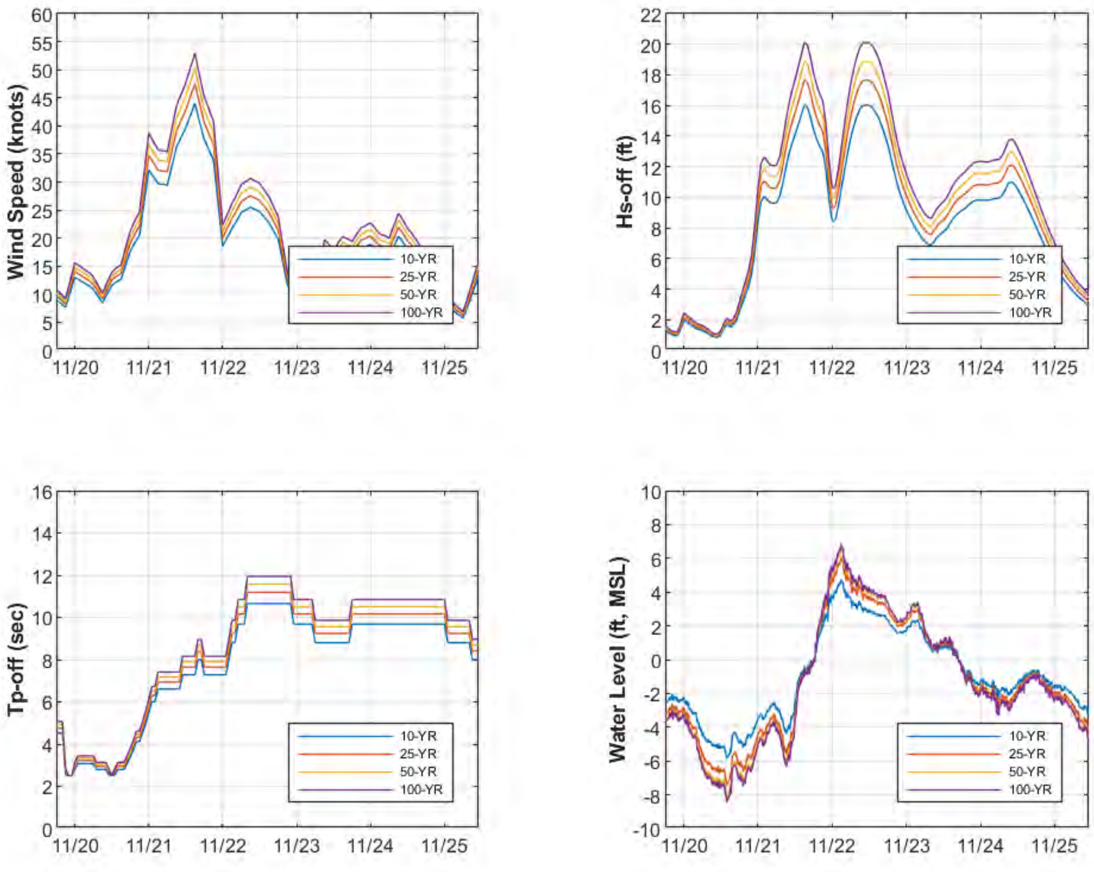

Figure 22. Scaled extreme event (Nov. 2017) for nearshore wave modeling

Table 8. Maxima of extreme events for nearshore wave modeling

Return Periods	Wind Speed (knots)	Significant Wave Height (ft)	Peak Wave Period (sec)	Water Level (ft, MSL)
10-year	44	16	10.7	4.8
25-year	47.6	17.7	11.2	6.1
50-year	50.3	18.9	11.6	6.7
100-year	53	20.1	11.9	6.9

The wave height/period and water level are applied uniformly along the offshore boundary of the model. Wind forcing is applied uniformly over the model domain. RSL change is introduced as an initial water level applied uniformly over the domain. The high RSL values in Table 7 are used for modeling.

Model output parameters from these simulations include significant wave height, maximum wave height, peak wave period, and mean wave direction. Output over the model domain is generated at 15-minute intervals, while output at the six nearshore locations is generated at 1-minute intervals. The nearshore output locations are positioned parallel to and approximately 160 ft from the shoreline (zero contour) as shown in Figure 23.

Figure 23. Nearshore output locations in MIKE 21 SW model

For illustration and discussion, Figure 24 presents the model results from simulating the 100-year event with 2050 RSL change, showing significant wave heights at the peak of the event. Wave heights are observed to decrease as they approach the shoreline fronting the airstrip, which is indicative of depth-limited wave breaking. This is consistent with observations in USACE (1998) and R&M (2018) regarding shallow bathymetry in the nearshore causing wave heights to be depth limited. Wave heights are higher at the south end of the barrier island (Loc-1 and Loc-2) than along the airstrip because the water depth is greater. Wave heights continue to decrease north of the city along the length of the airstrip (Loc-3 to Loc-6), but the difference is relatively small. These observations are true for all simulations.

As nearshore wave heights are fairly consistent along the airstrip, only output from Loc-3 is presented and used for analysis of the airstrip revetment. The maximum values of Hs and associated Tp at Loc-3 for all the nearshore wave simulations are summarized in Table 9.

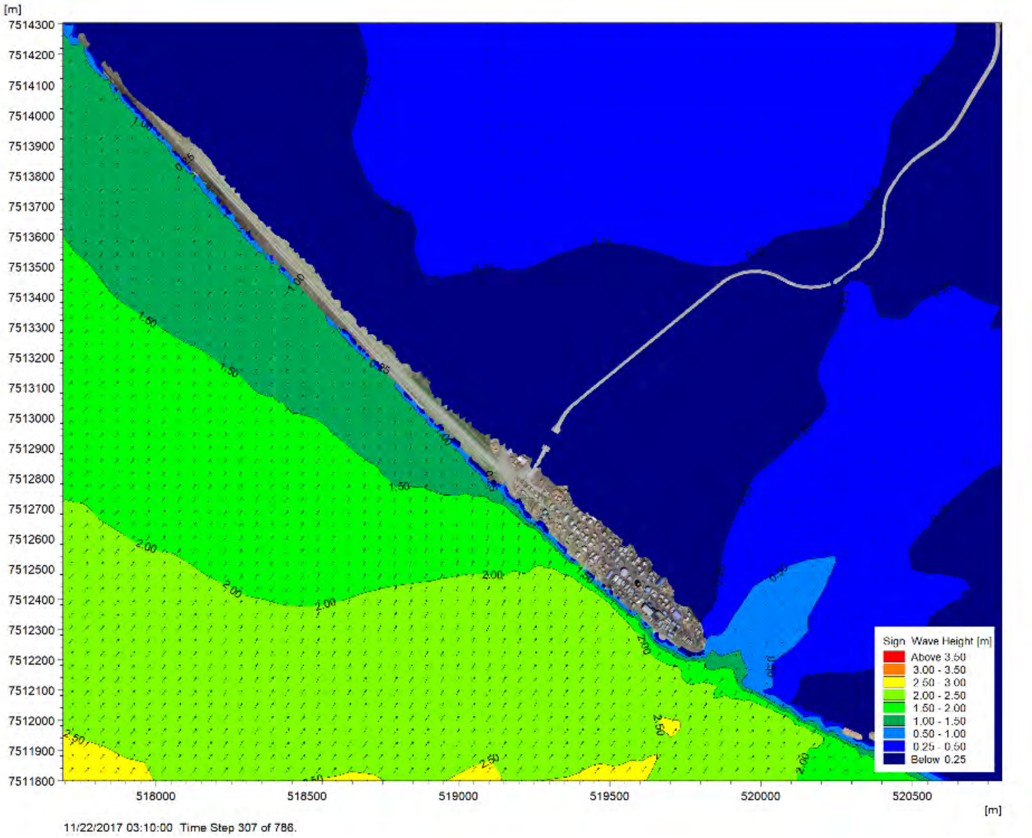

Figure 24. Significant wave heights (Hs) at the peak of event (100-year, 2050 RSL)

Table 9. Maximum nearshore waves from extreme events at Loc-3

RSL Projection (year)	RSL (ft)	Significant Wave Height, Hs (ft)				Peak Wave Period, Tp (sec)			
		10-yr	25-yr	50-yr	100-yr	10-yr	25-yr	50-yr	100-yr
Present	0.00	2.66	3.33	3.64	3.75	8.60	9.2	9.37	9.61
2050	1.20	3.25	3.91	4.22	4.33	8.60	9.22	9.38	9.61
2075	3.25	4.22	4.88	5.18	5.31	8.60	9.21	9.38	9.60
2100	6.32	5.59	6.25	6.57	6.70	8.59	9.21	9.39	9.61

5.3.2 Inundation Mapping: Extreme Events

The objective of these simulations is to produce inundation maps of the barrier island from extreme events in the present and considering RSL change in 2050, 2075, and 2100. The HD module is used to simulate flooding of areas typically above water and is coupled with the SW module to account for wave setup in the nearshore.

Figure 25 presents the inundation map for the 100-year event and 2050 RSL change, showing the maximum water depth at each node over the entire simulation period. Inundation maps for all modeled scenarios are presented in Appendix A.

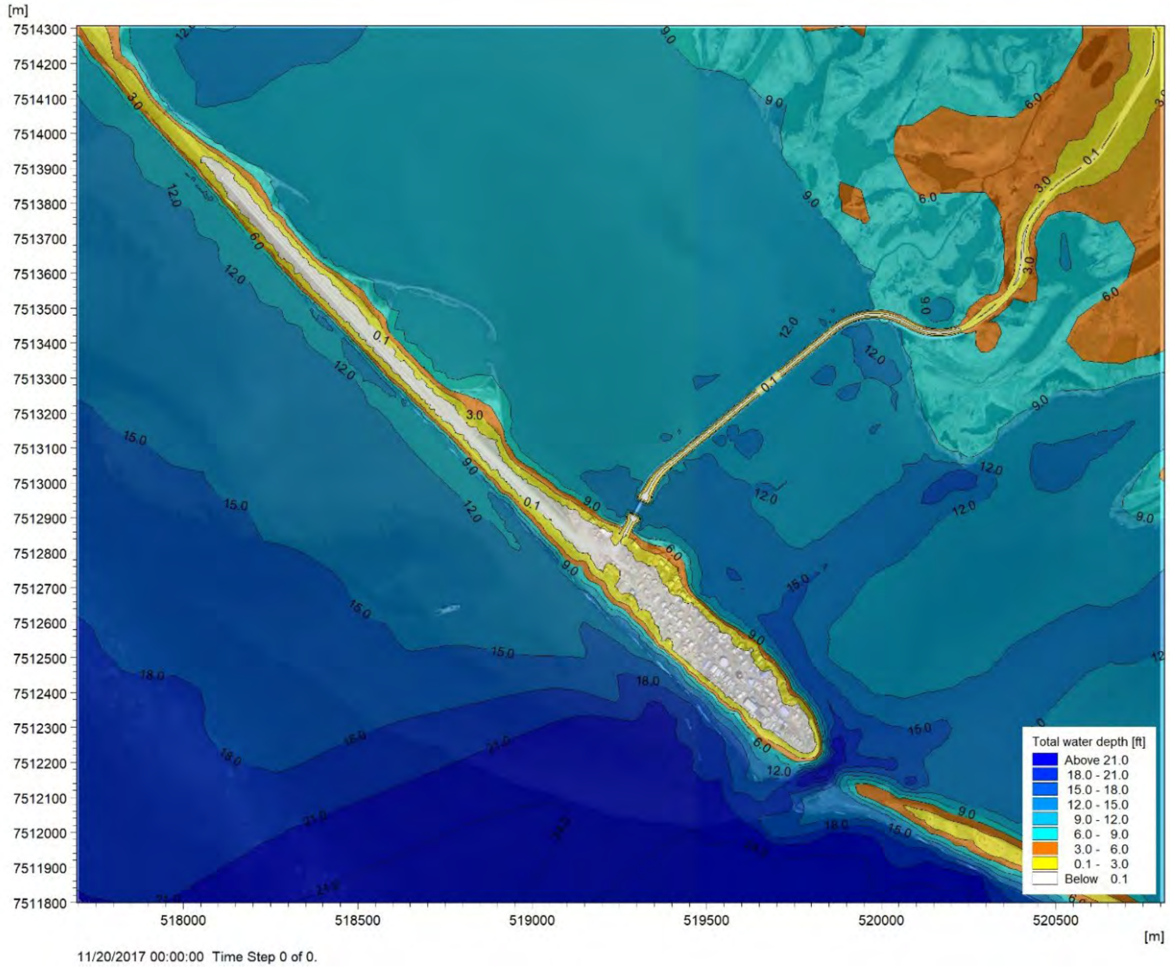

Figure 25. Maximum water depth for 100-year event and 2050 RSL change

The inundation maps provide insight on the vulnerability of the existing airstrip to flooding in the near future due to RSL change. The existing revetment has a top elevation of 16 ft NAVD88. The inundation maps suggest the following:

- In present day and in 2050, the runway is above the inland inundation extent for all events considered.
- In 2075 and events equal to or greater than 50-year, the inland inundation extent reduces the width of the runway.
- In 2100, the runway is completely inundated with up to 3 ft of water for all events.

The City of Kivalina is generally lower in elevation compared to the runway. The observations above therefore also apply to the city. The difference is that most of the city would be flooded by 2075 for events equal to or greater than 25-year.

5.3.3 Generalized Storm Conditions

The simulations consist of modeling a matrix of water levels, offshore waves and winds that covers a range of conditions characteristic of fall and winter storms based on analysis of the peak events in the WIS record. The results provide input to the damage progression analysis described in Section 6.2. The generalized storm characteristics are as follows:

- Increasing wind speed results in increasing wave height. Storm winds range from 20 – 50 knots and drive wave heights between 5 – 20 ft in the offshore region.
- Relatively steady wave periods varying from 5 – 10 seconds.
- Storm surge is relatively small, ranging from 2.5 – 5 ft.
- Offshore wind and wave direction can vary significantly from south to northwest. However, offshore wind and wave direction are aligned.

Table 10 presents the matrix of parameters. The water levels considered are 2.5 and 5.0 ft (MSL) and are applied uniformly in time and space The wind speed is varied from 20 to 50 knots. The offshore Hs is varied from 3.3 to 19.7 ft (1 to 6 m in 0.5 m increments). The peak wave period is kept constant at 10 sec. The offshore wind and wave direction are kept constant at 230 °N which is approximately normal to the Kivalina barrier island. The damage progression analysis is based on normal wave angle of attack and, therefore, these simulations align with that methodology.

Table 10. Matrix of generalized storm conditions for modeling

Water Level (ft, MSL)	Wind Speed (knots)	Wind Dir (°N)	Offshore Hs (ft)	Offshore Tp (sec)	Mean Wave Dir (°N)
2.5 and 5.0	20	230	3.3	10	230
	23	230	4.9	10	230
	26	230	6.6	10	230
	29	230	8.2	10	230
	32	230	9.8	10	230
	35	230	11.5	10	230
	38	230	13.1	10	230
	41	230	14.8	10	230
	44	230	16.4	10	230
	47	230	18.0	10	230
	50	230	19.7	10	230

The correlation between offshore and nearshore Hs from the generalized storm conditions is presented in Figure 26. The results confirm that depth-limited conditions govern in the nearshore region due to shallow depths.

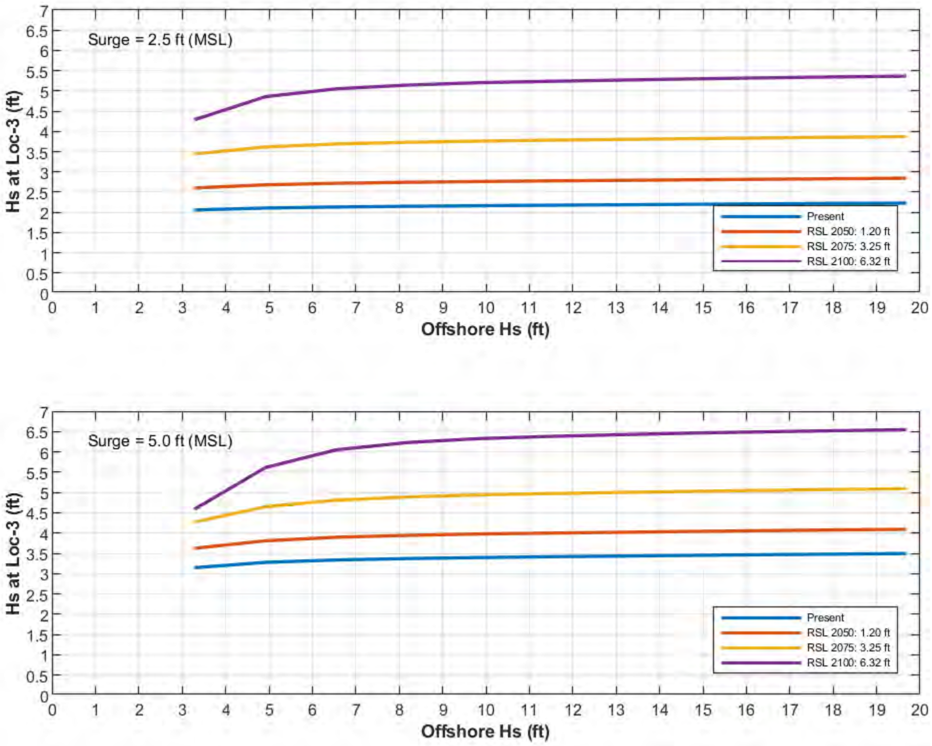

Figure 26. Results from generalized storm conditions

6.0 REVETMENT ANALYSES

6.1 ARMOR STONE SIZE

The armor stone weight of the existing revetment (M_{50} = 2,000 lb) was determined using the Hudson formula with the design parameters given in Table 1. The Hudson formula for irregular, head-on waves is (USACE, 2011):

$$M_{50} = \frac{\rho_s H_s^3}{K_D (\frac{\rho_s}{\rho_w} - 1)^3 cot\alpha}$$

H_s = Significant wave height

M_{50} = Equivalent cube length of median stone

ρ_s = Mass density of stone

ρ_w = Mass density of water

cot(α) = Cotangent of slope angle

K_D = Stability coefficient

The Hudson formula is utilized to estimate the armor stone median weight with the nearshore wave heights obtained from the simulation of extreme events with the SW model (Table 9). The results are presented in Table 11.

Table 11. Required armor stone weight based on maximum nearshore wave heights

RSL Projection (year)	RSL (ft)	Median Armor Stone Weight, M_{50} (lb)			
		10-yr	25-yr	50-yr	100-yr
Present	0.00	158	310	405	442
2050	1.20	288	502	631	681
2075	3.25	631	975	1,166	1,256
2100	6.32	1,466	2,048	2,379	2,523

The results indicate that the existing revetment (M_{50} = 2,000 lb) meets the requirement for approximately up to a 25-year storm event in 2100. Methods like Hudson and van der Meer, which are commonly used in the industry to design new revetments, provide the required armor stone weight to withstand the peak wave conditions of a single, specific design storm. However, a coastal revetment will experience a variety of events during its life, resulting in progressive damage that is not accounted for in the traditional armor stone stability methods. The next section presents an analysis of damage progression on the airstrip revetment to account for the exposure of the revetment to events of variable wave conditions to estimate the remaining life of the structure.

6.2 DAMAGE PROGRESSION

Damage progression is analyzed using the method described in Melby (2005), which is applicable to revetments exposed to depth-limited wave conditions. Damage is defined in terms of the average normalized cross-sectional eroded area of armor on the slope (A_e in Figure 27), up to the point that the underlayer is exposed through a hole equal in size to the nominal armor stone diameter (D_{n50}).

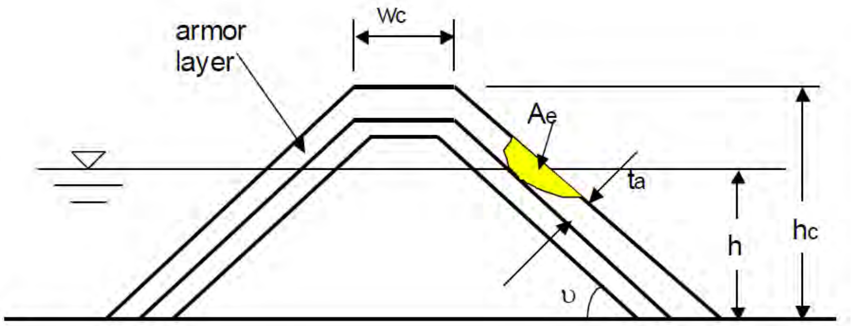

Figure 27. Cross-sectional eroded area (*A_e*) due to wave attack (Melby, 2005)

Damage is predicted by the following equation:

$$\bar{S}(t) = \bar{S}(t_n) + 0.022 \frac{(N_s)_n^5}{(T_p)_n^{0.25}} (t^{0.25} - t_n^{0.25}) \quad for \quad t_n \le t \le t_{n+1} \qquad Equation\ (1)$$

$\bar{S}(t)$ is predicted mean eroded area at time t

$\bar{S}(t_n)$ is known mean eroded area at time t_n (with $t > t_n$)

N_s is stability coefficient = $H_s/(\Delta D_{n50})$

H_s is significant wave height

Δ is relative density

D_{n50} is nominal armor stone diameter

T_m is mean wave period

The equation estimates damage over a sequence of N events. Each event has constant wave conditions over the period from t_n to t_{n+1} where $1 \le n \le N$. Waves are assumed to be normal to the revetment.

Melby (2005) does not comment on what damage values constitute initial, intermediate, and severe damage. It is our understanding that criteria provided in the Coastal Engineering Manual (CEM) can be applied to the results obtained from Equation (1). These criteria are presented in Figure 28.

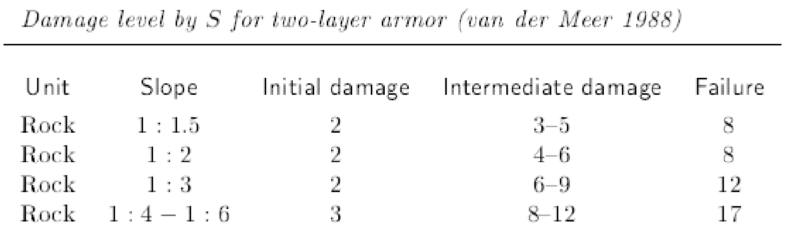

Damage level by S for two-layer armor (van der Meer 1988)

Unit	Slope	Initial damage	Intermediate damage	Failure
Rock	1 : 1.5	2	3–5	8
Rock	1 : 2	2	4–6	8
Rock	1 : 3	2	6–9	12
Rock	1 : 4 − 1 : 6	3	8–12	17

Figure 28. Damage level classification (USACE, 2011)

6.2.1 Validation

To validate the application of the Melby (2005) method to the damage progression analysis of the airstrip revetment, the damage progression from a physical experiment conducted by Melby and Kobayashi (1998) was reproduced. The experiment is referred to as Series A' and consists of six consecutive events "intended to define the long-term response of a structure." Figure 29 presents the results, showing that the implementation of the method is reasonably accurate. One source of error in the curve produced by Stantec is from manually digitizing the damage curve from Melby and Kobayashi (1998).

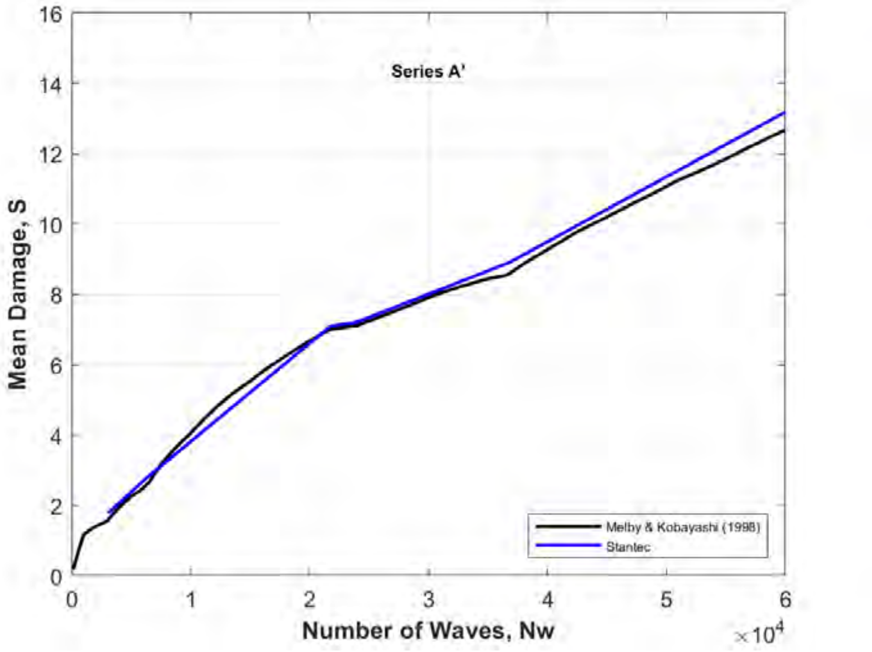

Figure 29. Validation of implementation of Melby (2005) method

6.2.2 Application

The definition and selection of events is the basis of the damage progression analysis. An event is defined by constant wave conditions represented by a significant wave height, peak wave period, and duration. The intent is to analyze the damage incurred by many events of varying wave conditions that are representative of conditions the revetment may endure during its design life.

The design life of the existing airstrip revetment is unknown. The revetment around the south end of Kivalina, which was completed in 2010, has a 15-year project life (USACE, 2007) because the city was planning to relocate within that time frame. The damage progression analysis is carried out for a period of 20 years.

The offshore data from WIS ST82059 is an appropriate source of long-term, varying wave conditions from which to identify events and process them for use in the damage progression analysis. The selection of events is based on the following process:

1. A damage-causing event is defined by periods of offshore Hs ≥ 10 ft and a minimum duration of 12 hours. As discussed in Section 3.1.2, the storms that generate the most adverse conditions along the Alaskan coastline of the Chukchi Sea move slowly and their impact on the coastline is of scale of days. Also, a short event will not generate appreciable storm surge at the coastline. For this reason, events with lower wave heights and shorter duration are not considered, as they will theoretically inflict damage on the revetment with the use of Equation (1) and result in overestimation of cumulative damage.

   From this screening:

   a) The number of events in each year of the WIS record is calculated. From this vector, the mean (μ_{NE}) and standard deviation (σ_{NE}) of the number of events per year are calculated. These statistics are presented in Table 12.

   b) The mean (μ_{PK}) and standard deviation (σ_{PK}) of the peak wave height in each event is calculated. These statistics are presented in Table 12.

Table 12. Statistics calculated from WIS record

WIS ST82059	Events/Year		Peak Wave Height (ft)	
	μ_{NE}	σ_{NE}	μ_{PK}	σ_{PK}
Present	2.7	1.7	12.2	1.8
Future (ice-free)	3.6	1.9	12.0	1.7

2. The number of events in each year (20 years total) is randomly drawn from the normal distribution specified by the corresponding mean and standard deviation (μ_{NE} and σ_{NE}, respectively).

3. The damage progression analysis then proceeds by individual years. Suppose that 4 events are assigned to year 1. The offshore wave conditions for each event of the 4 events are determined as follows, using event 1 as an example:
    a) The peak wave height for event 1 is randomly drawn from the normal distribution specified by the corresponding mean and standard deviation (μ_{PK} and σ_{PK}, respectively).
    b) Based on the randomly selected peak wave height, events in the WIS record identified in Step 1 with the closest peak wave height are gathered. A random number generator is then used to select a single event from the group. This is an event extracted from the WIS record (i.e., time series of offshore wave height and period with Hs ≥ 10 ft).
    c) The use of Equation (1) requires the events to have constant wave conditions. This is accomplished by averaging the Hs and Tp of the event. An average storm surge of 2.5 ft is assumed.
    d) Event 1 is now defined in terms of an average offshore wave height and peak wave period. The results from the Generalized Storm Conditions (Section 5.3.3) are used to translate the offshore wave height to a nearshore wave height. The peak wave period is assumed to remain constant as the wave propagates from offshore to nearshore.
    e) Event 1, now defined by nearshore wave conditions, is used as input to Equation (1). The cumulative mean damage from event 1 becomes the initial damage for event 2.
4. Step 3 is applied to years 1 to 20.
5. The simulation of the 20 years is repeated 10,000 times (which is typically required in a Monte Carlo simulation) to generate consistent results given the various randomized selection processes.
6. Finally, exceedance curves are developed for mean damage at 5, 10, 15, and 20 years, using the results from the 10,000 simulations.

Figure 30 and Figure 31 present the exceedance curve for present (with sea ice) and future (without sea ice) conditions, respectively. According to the damage classification in Figure 28, damage equal to or greater than 8 constitutes failure for a revetment with a 1V:1.5H slope. The following conclusions about the existing airstrip revetment are therefore drawn from the exceedance curves.

Present sea ice cover conditions:

- The revetment will experience intermediate damage but will not fail in the next 5 years.
- There is a 1% chance that the revetment will fail in the next 10 years.
- There is a 50% chance that the revetment will fail in the next 15 years.

- There is a 97% chance that the revetment will fail in the next 20 years.

Without sea ice cover conditions:

- The revetment will experience intermediate damage but will not fail in the next 5 years.
- There is a 25% chance that the revetment will fail in the next 10 years.
- There is a 75% chance that the revetment will fail in the next 15 years.
- The revetment will fail in the next 20 years.

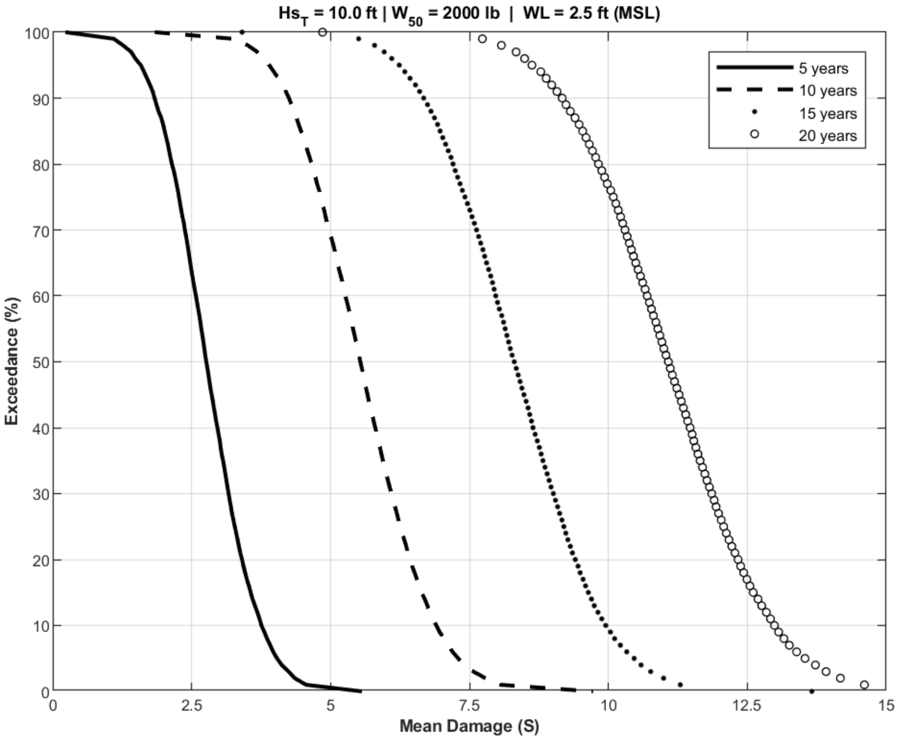

Figure 30. Revetment damage progression exceedance curve for present sea ice conditions

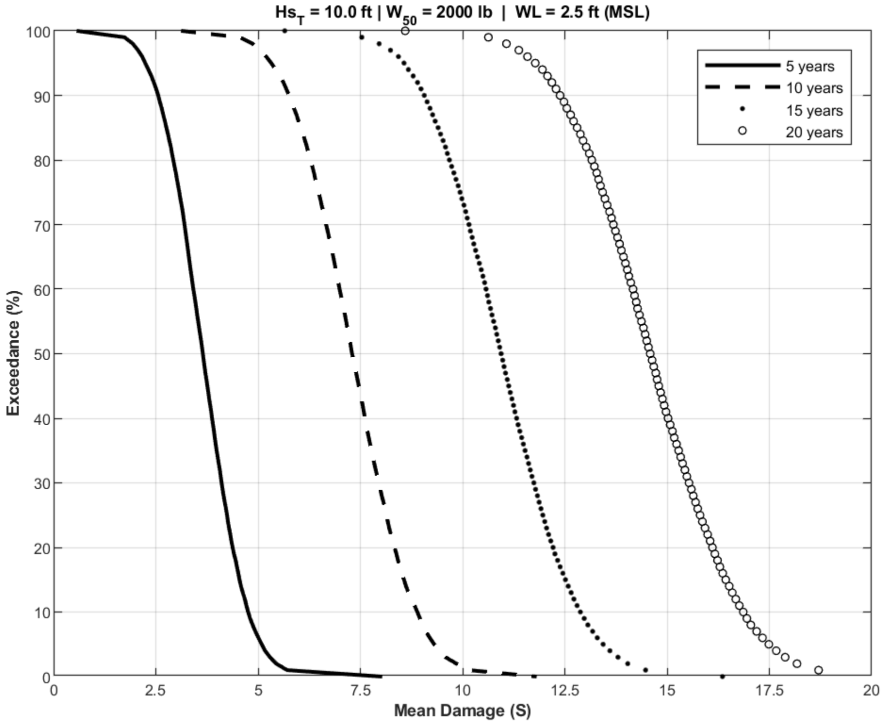

Figure 31. Revetment damage progression exceedance curve for future sea ice conditions

The results of the damage progression analysis indicate that the existing airstrip revetment may experience failure in the next 10 – 15 years. These results are accompanied by the following assumptions:

- Damage is solely caused by waves. Damage caused by ice pushed against the revetment is not included in the analysis.
- Maintenance and repair works are not performed on the revetment.
- The difference between present and future sea ice conditions is accounted for only in the probability of an event occurring, with the probability being higher for future sea ice conditions because of the lack of sea ice. It can be argued that global warming effects may increase wind speeds and wave heights in the future; however, the analysis does not include this potential effect of global warming.
- Waves are assumed to be normal to the revetment. The damage progression calculation method does not include wave directionality.

- The revetment is assumed to experience damage equally along its length. However, it is possible that some reaches will deteriorate faster than others, if nearshore bathymetry and beach conditions become variable along the revetment.

7.0 ALTERNATIVES ANALYSIS

The performance of the revetment and stability of the runway may be improved by the following alternatives.

1. Alternative 1: Additional Armor Stone. Failure of a revetment is defined by exposure of the filter layer. Adding stone to the existing revetment will provide an additional layer of protection from waves and should extend the service life. The additional stone shall be equal to or greater in size/weight than the existing stone. The thickness of the layer shall be at least equal to one nominal stone diameter (D_{n50}) and follow the slope and geometry of the existing revetment from the crest to the toe. Figure 32 shows a schematic of this alternative. Based on engineering judgement, Alternative 1 could add 5 to 10 years of useful life to the revetment but would not protect the runway from flooding.

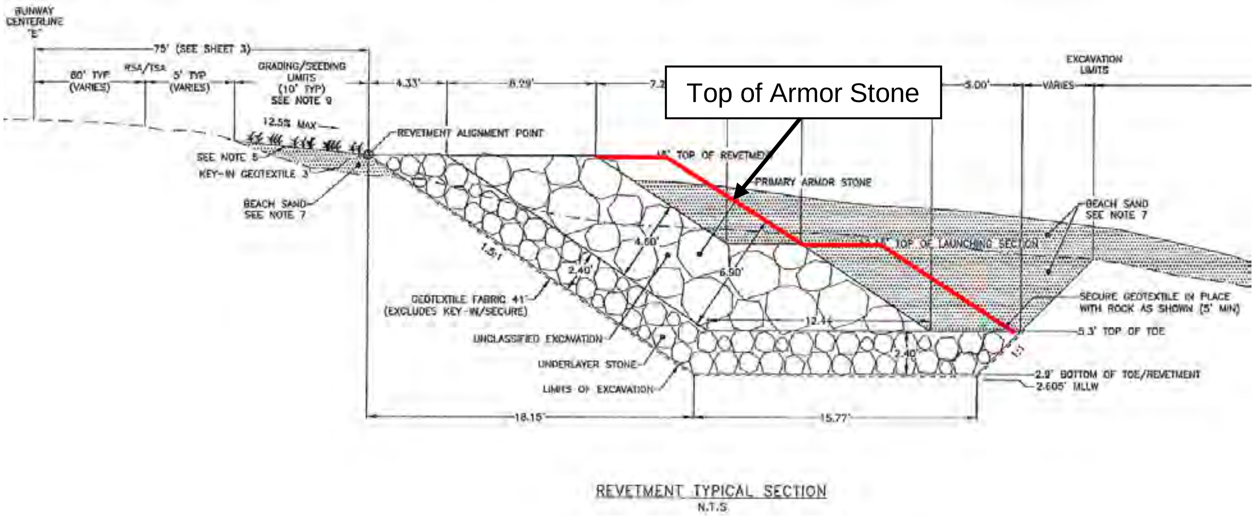

Figure 32. Alternative 1: Additional armor stone

2. Alternative 2: Raising the Runway. This alternative consists of raising the grade to minimize damage to the runway associated with wave overtopping. Raising the runway would also require a commensurate extension of the revetment, both filter and armor stone layers, as shown in Figure 33.

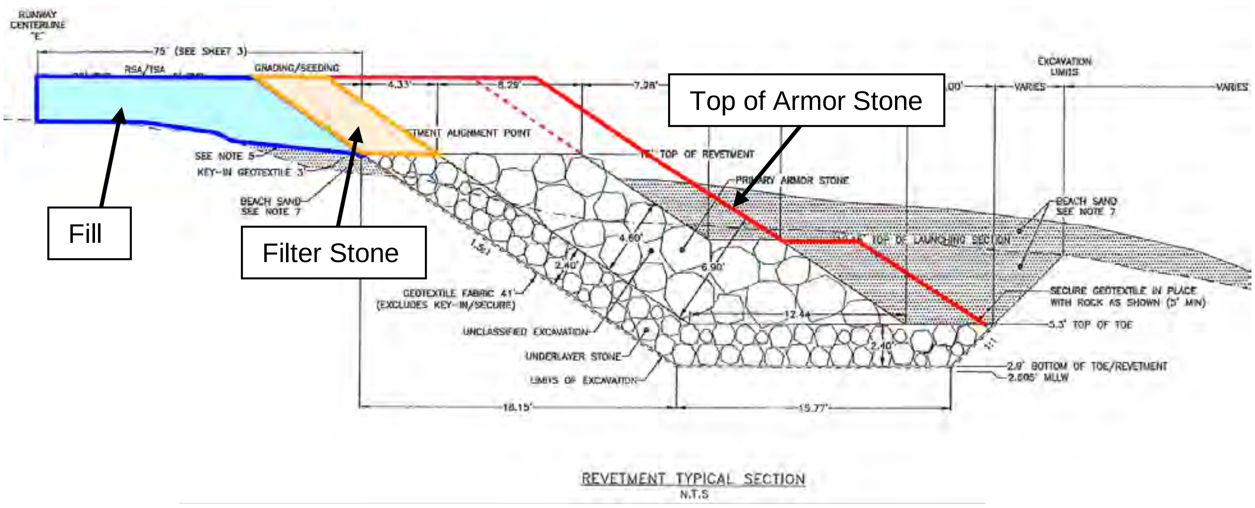

Figure 33. Alternative 2: Raising the runway and placing additional armor stone

A freeboard is often included in determining the elevation of structures in coastal areas vulnerable to flooding. For levees located in coastal areas, the Federal Emergency Management Agency (FEMA) specifies a 1-ft freeboard above the height of the one percent wave or the maximum wave runup (whichever is greater) associated with the 100-year event (FEMA, 2020). Based on the results from the extreme event simulations (Section 5.3.2), the required runway elevations are presented in Table 13, applying a 1-ft freeboard consistently from the 10-year to the 100-year event and rounding up to the nearest 0.5 ft.

Table 13. Required runway elevation including a 1-ft freeboard

SLR Projection (year)	SLR (ft)	Required Runway Elevation (ft, NAVD88)			
		10-yr	25-yr	50-yr	100-yr
2050	1.20	16	16	16	16
2060	1.89	16	16	16	16
2075	3.25	16	17	17.5	18
2100	6.32	19	20.5	21	21

Based on discussion with the Alaska DOT&PF, results are presented for year 2060, assuming a 25-year design life with year 2035 as the base year. Model results for this condition are not readily available; however, the assessment is based on results for years 2050 and 2075. The results suggest that the freeboard requirement is met at the existing elevation of +16 ft NAVD88 for a 100-year event in year 2060. As a check, wave overtopping is calculated using Equation 5.16 of the EurOtop Manual II (Van der Meer et al., 2018) which is an equation applicable to shallow foreshores such as the foreshore in Kivalina. Evaluation of the 100-year conditions

(Table 9) with sea level rise in 2060 and a runway elevation of +16 ft NAVD88 result in zero wave overtopping.

Raising of the runway could be achieved without adding armor stone beyond the existing horizontal extent (dashed line in Figure 33). However, raising the runway does not add stability to the revetment itself; therefore, the additional layer of armor stone would provide an extra layer of protection against damage from waves. Based on engineering judgement, Alternative 2 could add 5 to 10 years of useful life to the revetment with the additional benefit of preventing flood-related impacts to the runway.

3. Alternative 3: Improving Beach Stability. Improvement to the beach stability can be gained by the addition of groins, which can be used in combination with Alternatives 1 and 2.

   Groins are shore-perpendicular structures, commonly made of heavy armor stone, which interfere with longshore sediment transport, creating sediment accretion on the updrift side and erosion on the downdrift side that creates a fillet-shaped shoreline following equilibration. The erosion on the downdrift side is of particular note for Kivalina, as can be seen at the Red Dog port, erosion could further threaten the viability of current infrastructure.

   It is anticipated that at least two groins may be required at Kivalina, as shown in Figure 34. A more detailed analysis involving numerical modeling of sediment transport is required to determine the most optimal position and length of the groins and any impacts to adjacent shorelines.

   Considering the proximity of the inlet connecting the Chukchi Sea to the Kivalina Lagoon (known as Singalliik Entrance), jetties to either side of the inlet may be required to protect it from the effects that the proposed groins will have on local sediment transport that could potentially cause shoaling of the inlet. The need, optimal orientation and length of the jetties would also require additional analyses and numerical modeling. The jetties are exemplified in Figure 34.

   In addition to growing and stabilizing the beach, the groins and jetties will provide protection to portions of the Kivalina coastline from storm waves approaching at oblique angles, particularly from the SE and NW. The armor stone of the groins would therefore have to be sized accordingly.

Figure 34. Alternative 4: Groins (yellow) for beach stability and jetties (red) for inlet stability

Based on engineering judgement and without detailed sediment transport studies, Alternative 3 is not recommended, due to the uncertainties surrounding erosion downdrift of the groins.

4. Alternative 4: No Action. The analyses conducted in this report suggest that the size of the armor stone and overall design of the existing revetment are reasonable based on the storm conditions that the Kivalina coastline experiences. The damage progression analysis, which was conducted assuming no improvements to the revetment, suggests the revetment has 10 – 15 years before it experiences failure. The No Action alternative is viable if the airport is relocated, or the revetment is actively maintained, in the next 10 – 15 years.

In addition, the following works can improve the resiliency of the revetment in combination with Alternatives 1 – 2 and for Alternative 4.

(A) Performing maintenance and repair works in the summer months.

(B) Paving the runway. This would provide increased protection to the runway from wave runup and overtopping, especially as sea level rises.

(C) Stabilizing the back slope. Storm surge and sea level rise will increase the potential for overtopping of the revetment. During a storm, while the revetment may be stable, the back slope may erode and compromise the stability of the revetment. Currently, the back slope is vegetated in some areas. Placing armor stone on this slope will reduce the erosion potential. The armor stone on this slope can be smaller than the seaward revetment stone, as it will not experience direct wave attack.

8.0 CONCLUSIONS

According to the literature review and data analyses conducted in this study, the Kivalina airstrip revetment will be subject to more storms in the winter in the future, as global warming continues to reduce the spatial and temporal coverage of sea ice.

The results of the damage progression analysis indicate that the existing airstrip revetment will experience failure in the next 10 – 15 years, assuming damage is solely caused by waves and maintenance and repair works are not performed on the revetment.

Alternatives are proposed to extend the life of the revetment and increase protection to the runway, including adding a layer of armor stone to the face of the revetment, and adding a layer of armor stone to the face of the revetment and raising the runway (along with the revetment) based on the desired year and storm event (Table 13). The existing runway elevation of +16 ft NAVD88 is estimated to be sufficient to result in negligible wave overtopping of the runway for up to a 10-year event in year 2075, including a 1-ft freeboard. A third alternative involving new groins is discussed but it is not recommended at this time.

The No Action alternative is also discussed. The analyses conducted in this report suggest that the size of the existing armor stone and overall design of the existing revetment are reasonable based on the storm conditions at Kivalina. Assuming the airport is relocated in 10 – 15 years, or the revetment is actively maintained, the No Action alternative is viable.

The proposed alternatives and No Action alternative should also consider performing maintenance and repair works in the summer months, paving the runway, and stabilizing the back slope on the lagoon side.

9.0 REFERENCES

Alaska Department of Transportation & Public Facilities (DOT&PF). (1984). “Engineering Geology and Soils Report, Kivalina Airport.” Project No. D21332.

Alaska Department of Transportation & Public Facilities (DOT&PF). (2018). “Kivalina Airport Erosion Control As-Built Drawings.” Project No. Z638720000.

Alaska Department of Transportation & Public Facilities (DOT&PF). (2020). “Standard Specifications for Highway Construction.” https://dot.alaska.gov/stwddes/dcsspecs/assets/pdf/hwyspecs/sshc2020.pdf

DeGrandpre, K.G. (2015). “Relative Sea Level Change in Western Alaska Estimated from Satellite Altimetry and Repeat GPS Measurements.” M.S. Thesis, University of Alaska Fairbanks. https://scholarworks.alaska.edu/handle/11122/6076

DGGS. Alaska Tidal Datum Portal. Alaska Tidal Datum Portal | Alaska Division of Geological & Geophysical Surveys

DGGS Staff. (2015). Alaska Shoreline Change Tool: Alaska Division of Geological & Geophysical Surveys Digital Data Series 9, http://doi.org/10.14509/shoreline. https://doi.org/10.14509/29504

DOWL Engineers. (1994). “City of Kivalina, Alaska, Relocation Study.” Prepared for Kivalina City Council. https://www.commerce.alaska.gov/web/Portals/4/pub/1994_Kivalina%20Relocation%20Study.pdf

EurOtop, 2018. Manual on wave overtopping of sea defences and related structures. An overtopping manual largely based on European research, but for worldwide application. Van der Meer, J.W., Allsop, N.W.H., Bruce, T., De Rouck, J., Kortenhaus, A., Pullen, T., Schüttrumpf, H., Troch, P. and Zanuttigh, B., www.overtopping-manual.com.

Federal Emergency Management Agency (FEMA). (2020). “Guidance for Flood Risk Analysis and Mapping: Levees.” fema_levee-guidance.pdf

HDR. (2016). “Point Hope Coastal Erosion Study.” Prepared for the Alaska Department of Transportation & Public Facilities.

Huang, L., Wolcott, D., and Yang, H. (2012). “Tidal Characteristics Along the Western and Northern Coasts of Alaska.” Center for Operational Oceanographic Products and Services National Ocean Service/NOAA. https://legacy.iho.int/mtg_docs/rhc/ArHC/ArHC3/ARHC3-3.2.4_TidalCharacteristicsAK.pdf

Fang, Z., Freeman, P.T., Field, C.B., and Mach, K.J. (2018). “Reduced sea ice protection period increases storm exposure in Kivalina, Alaska.” Arctic Science, Vol. 4, No. 4. https://cdnsciencepub.com/doi/pdf/10.1139/AS-2017-0024

Melby, J. (2005). “Damage Development on Stone-Armored Breakwaters and Revetments.” ERDC/CHL CHETN-III-64. https://apps.dtic.mil/sti/pdfs/ADA441158.pdf

Melby, J. and Kobayashi, N. (1998). “Damage Progression on Breakwaters.” https://icce-ojs-tamu.tdl.org/icce/article/view/5731/5401.

National Oceanic and Atmospheric Administration (NOAA). (2004). “Erosion Study Report AK0302 Kivalina.”

National Oceanic and Atmospheric Administration (NOAA). (1998). “Automated Surface Observation System (ASOS) User’s Guide.” https://www.weather.gov/media/asos/aum-toc.pdf

Overland, J. (1981). “Marine Climatology of the Bering Sea.” In: D.W. Hood and J.A. Calder (eds.), The eastern Bering Sea shelf: Oceanography and resources, Vol. 1. NOAA. Distributed by the University of Washington Press, Seattle, pp. 15- 22. https://www.pmel.noaa.gov/pubs/docs/Eastern_Bering_1.2.pdf

Pingree-Shippee, K.A., Shippee, N., and Atkinson, D.E. (2016). “Overview of Bering and Chukchi Sea Wave States for Four Severe Storms following Common Synoptic Tracks.” Journal of Atmospheric and Oceanic Technology. https://journals.ametsoc.org/view/journals/atot/33/2/jtech-d-15-0153_1.xml?tab_body=abstract-display

R&M Consultants, Inc. (2018). “Design Narrative Memo, Kivalina Erosion Control Project.” Prepared for the Alaska Department of Transportation & Public Facilities.

Stabeno, P.J., Schumacher, J.D., and Ohtani, K. (1999). “The Physical Oceanography of the Bering Sea.” Dynamics of the Bearing Sea, Chapter 1.

Stantec. (2018): “Hydrodynamic Modeling Results in Support of Kivalina Lagoon Crossing Design.” Prepared for the Alaska Department of Transportation & Public Facilities.

Sweet. W., Kopp, R.E., Weaver, C.P., Obeysekera, J., Morton, R.M., Thieler, E.R., and Zervas, C. (2017). “Global and Regional Sea Level Rise Scenarios for the United States.” NOAA Technical Report NOS CO-OPS 083. https://ntrs.nasa.gov/api/citations/20180001857/downloads/20180001857.pdf

Tajima, Y., and Madsen, O. (2005). “Waves, Currents, and Sediment Transport in the Surf Zone along Long, Straight Beaches.” ERDC/CHL CR-05-01. https://dspace.mit.edu/bitstream/handle/1721.1/29441/56193320-MIT.pdf?sequence=2

U.S. Army Corps of Engineers (USACE). (1998). “Community Improvement Feasibility Report, Kivalina, Alaska.”https://www.poa.usace.army.mil/Portals/34/docs/civilworks/archive/commuityimprovementfeasibilityreportkivalina.pdf

U.S. Army Corps of Engineers (USACE). (2006). “AVETA Report Summary – Kivalina, Alaska.” https://www.poa.usace.army.mil/Portals/34/docs/civilworks/BEA/Kivalina_Final%20Report.pdf

U.S. Army Corps of Engineers (USACE). (2011). “Coastal Engineering Manual: Part VI - Chapter 5 Fundamentals of Design.” EM-1110-2-1100.

U.S. Army Corps of Engineers (USACE). (2016). “Causeway and Bridge Design Report.” Kivalina Lagoon Crossing Planning Assistance to States.

U.S. Army Corps of Engineers (USACE). (2020). “Condition of Improvements, 31 December 2019, Kivalina Coastal Erosion, Alaska.” CWIS No. 081818. https://www.poa.usace.army.mil/Portals/34/docs/operations/EFC/2019KivalinaOverview.pdf?ver=2020-04-30-171454-413

APPENDIX A

Maximum Inundation Depth of Coastal and Overland Flood Flows

Appendix A MAXIMUM INUNDATION DEPTH OF COASTAL AND OVERLAND FLOOD FLOWS

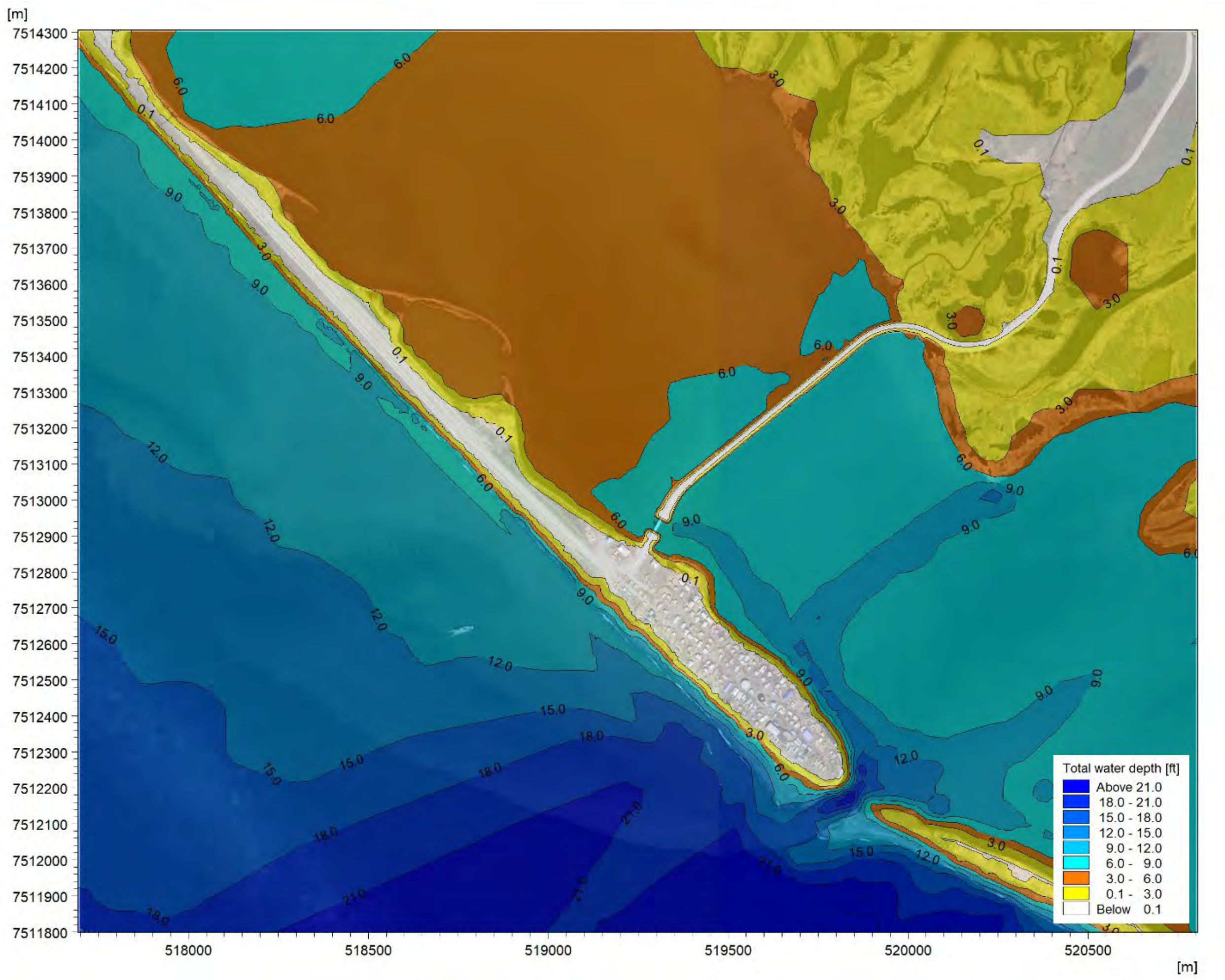

Figure A-1: Maximum Water Depth for 10 Year Event at No SLR (HDSW_C01)

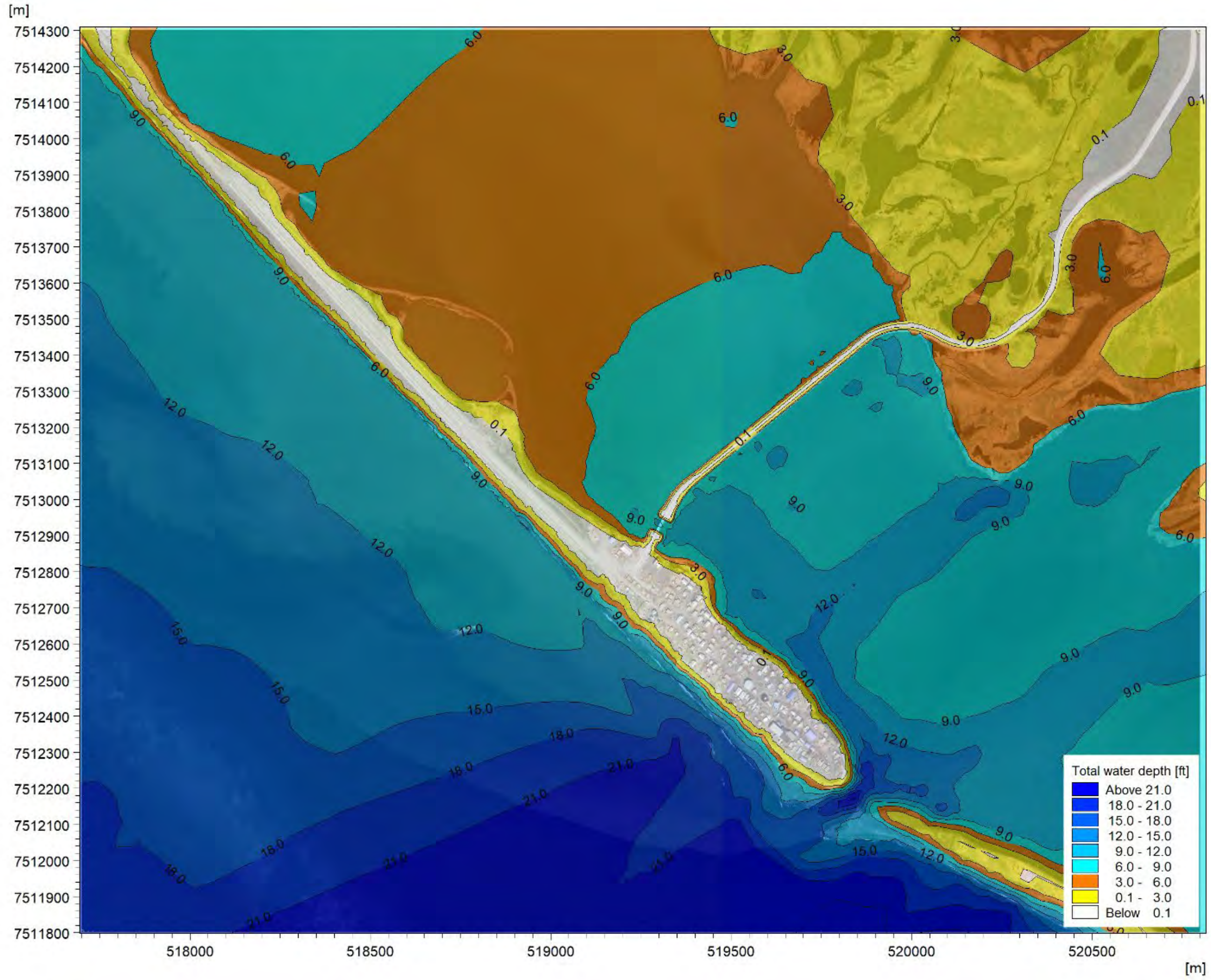

Figure A-2: Maximum Water Depth for 25 Year Event at No SLR (HDSW_C02)

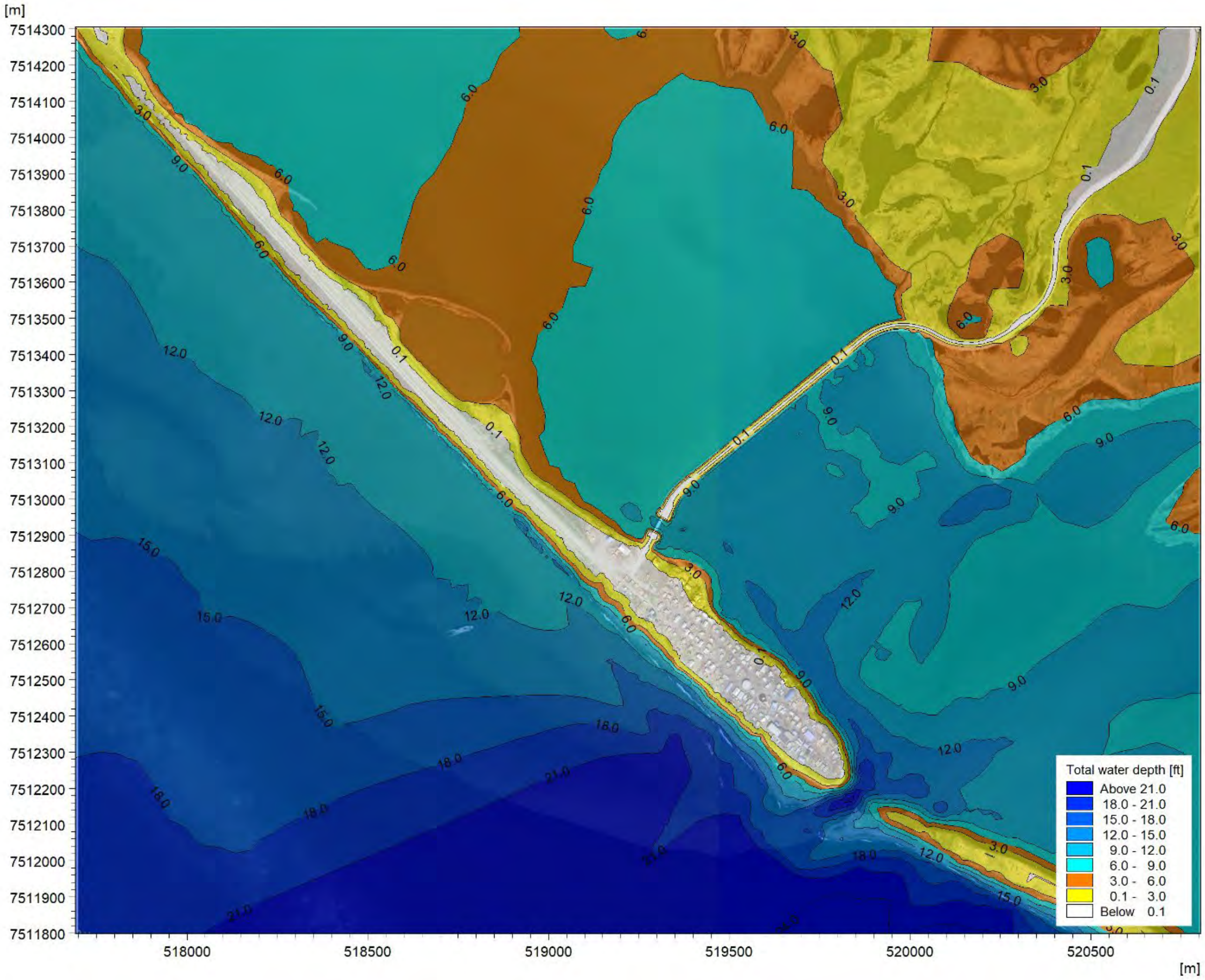

Figure A-3: Maximum Water Depth for 50 Year Event at No SLR (HDSW_C03)

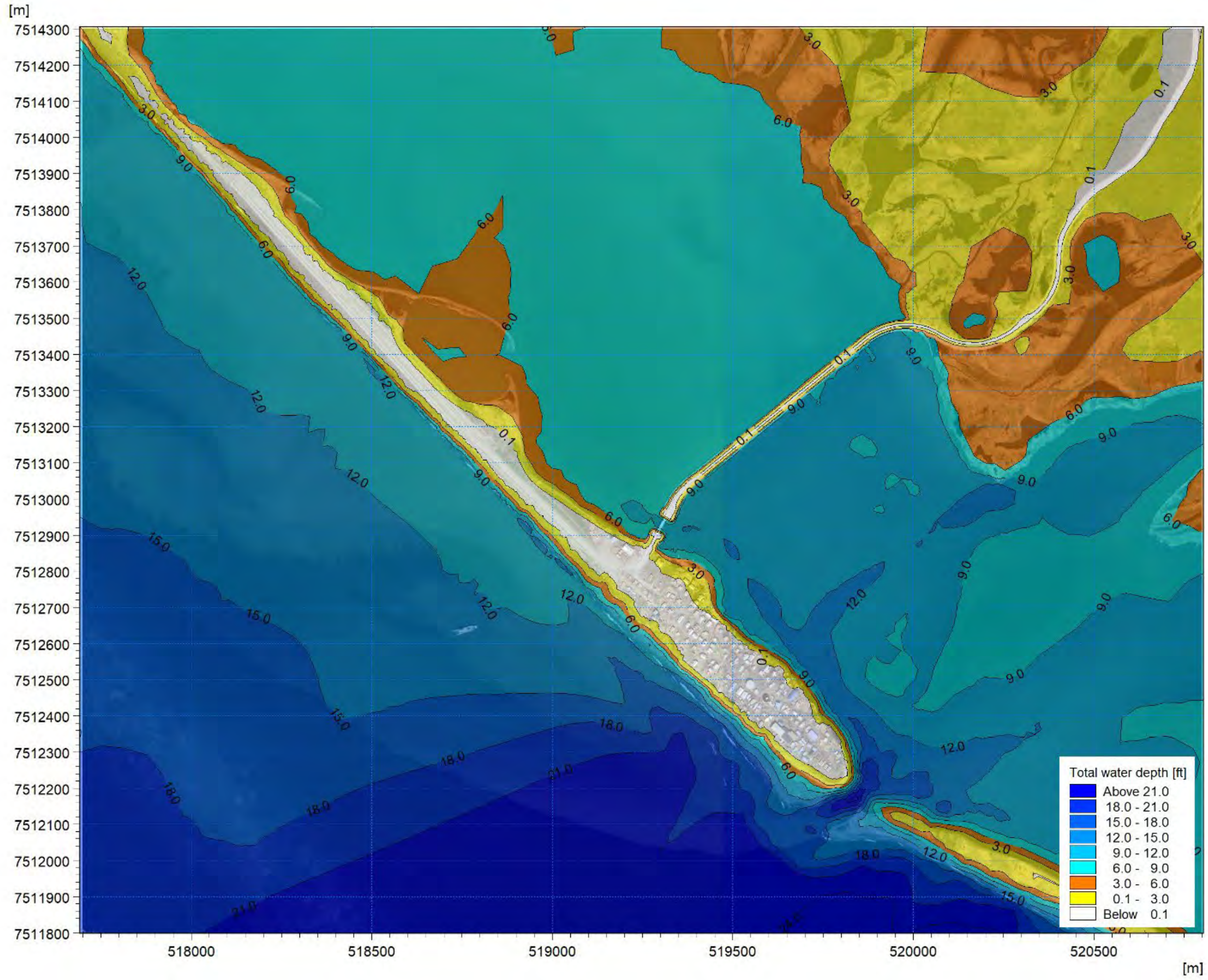

Figure A-4: Maximum Water Depth for 100 Year Event No SLR (HDSW_C04)

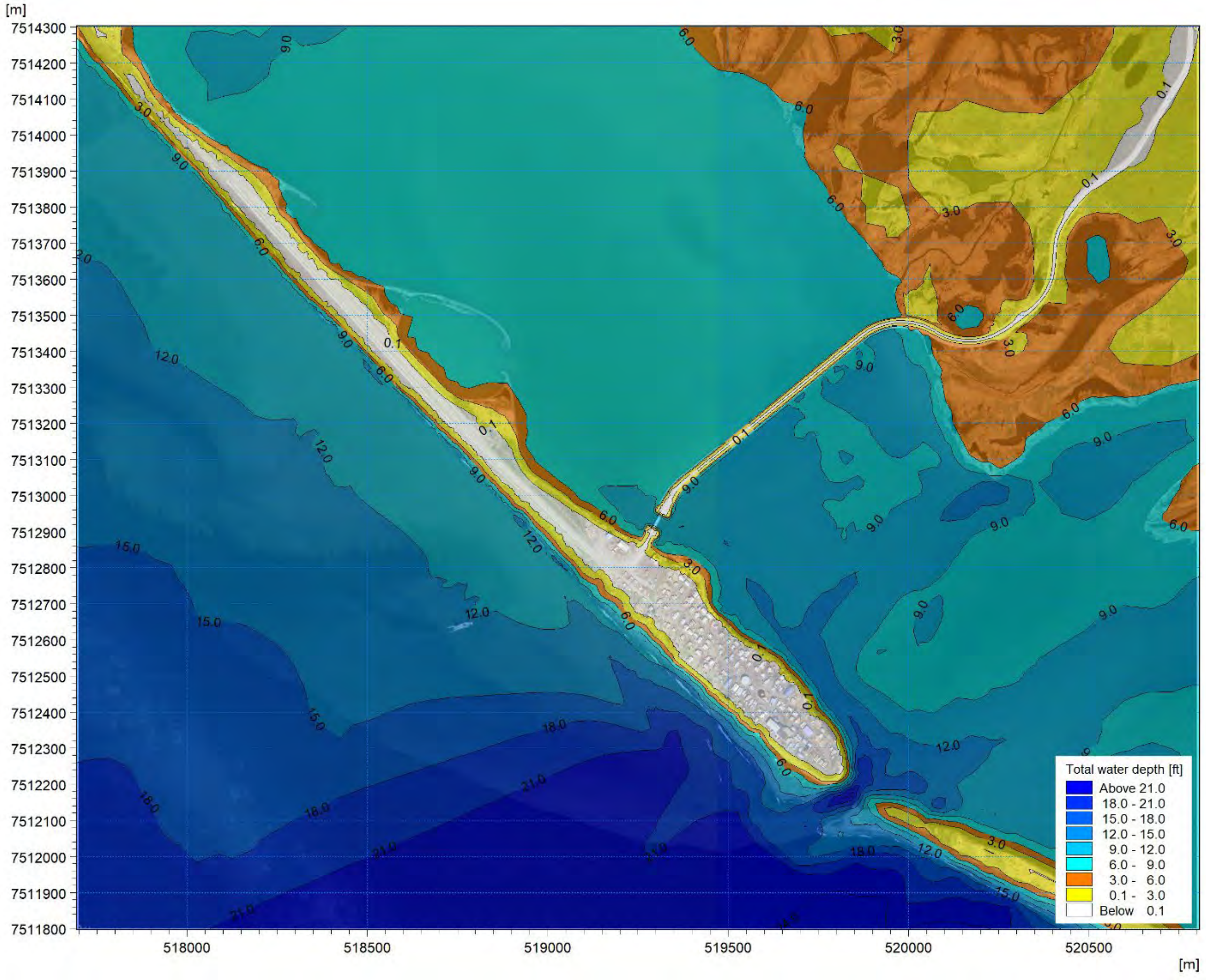

Figure A-5: Maximum Water Depth for 10 Year Event at SLR 2050 (HDSW_C11)

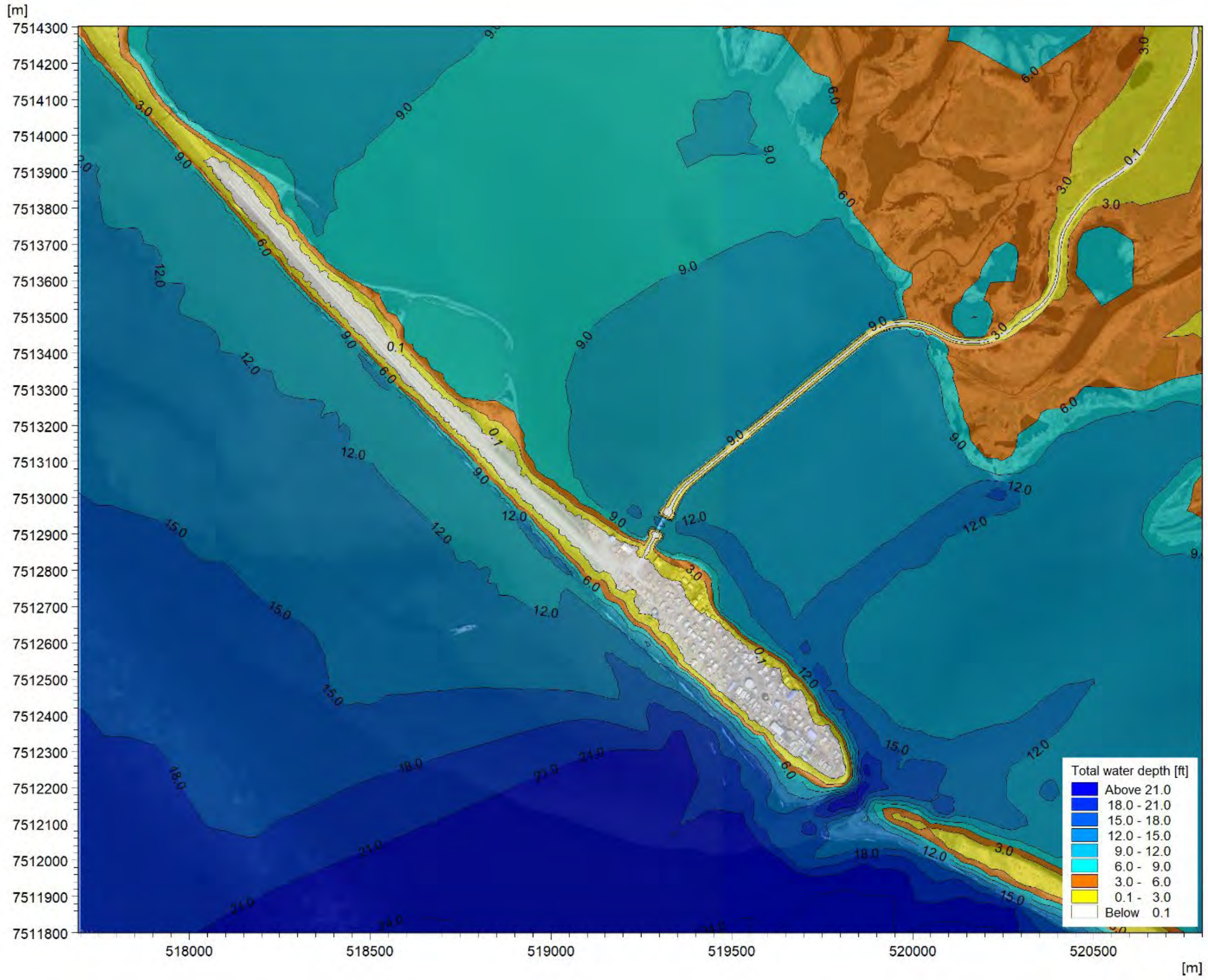

Figure A-6: Maximum Water Depth for 25 Year Event at SLR 2050 (HDSW_C12)

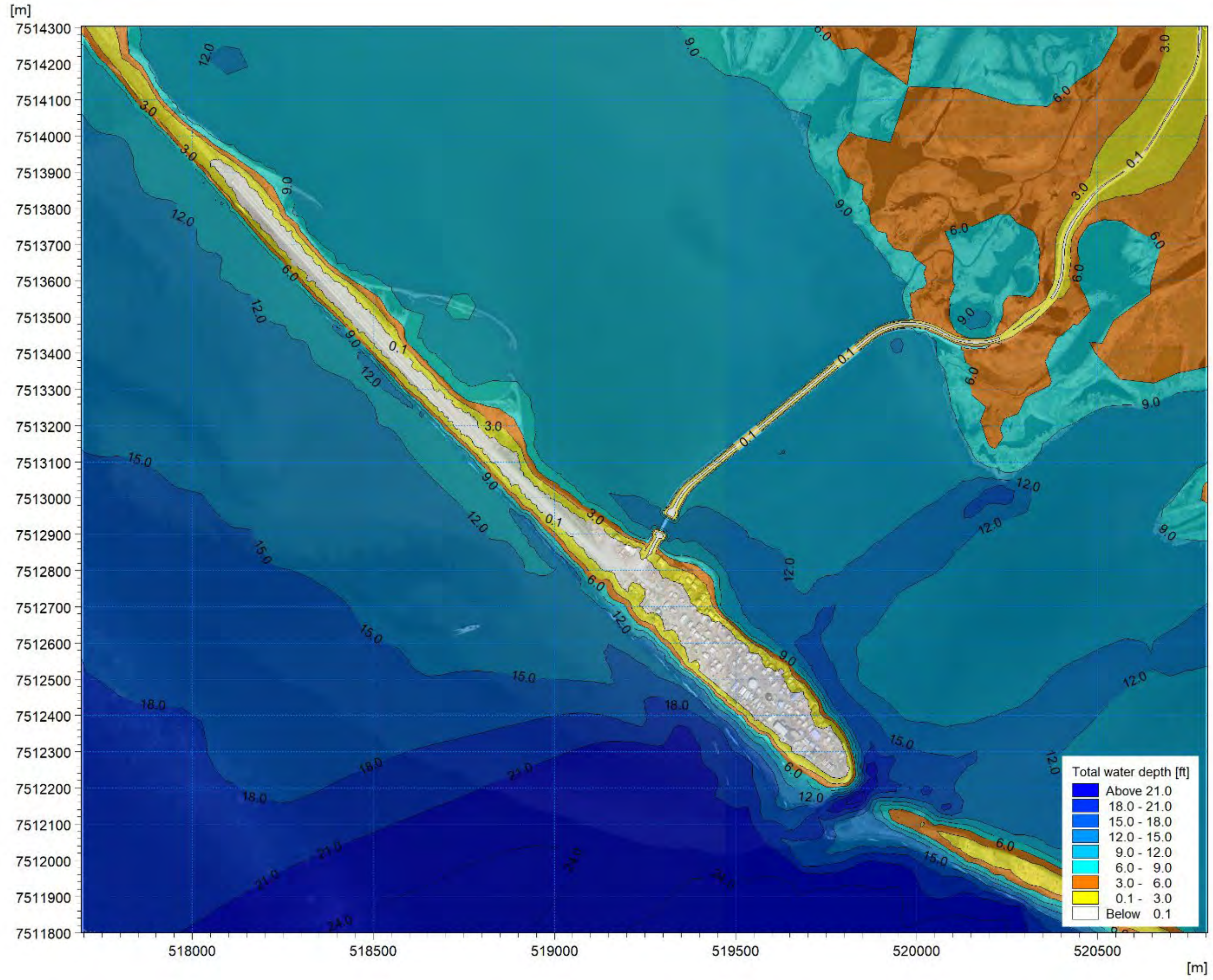

Figure A-7: Maximum Water Depth for 50 Year Event at SLR 2050 (HDSW_C13)

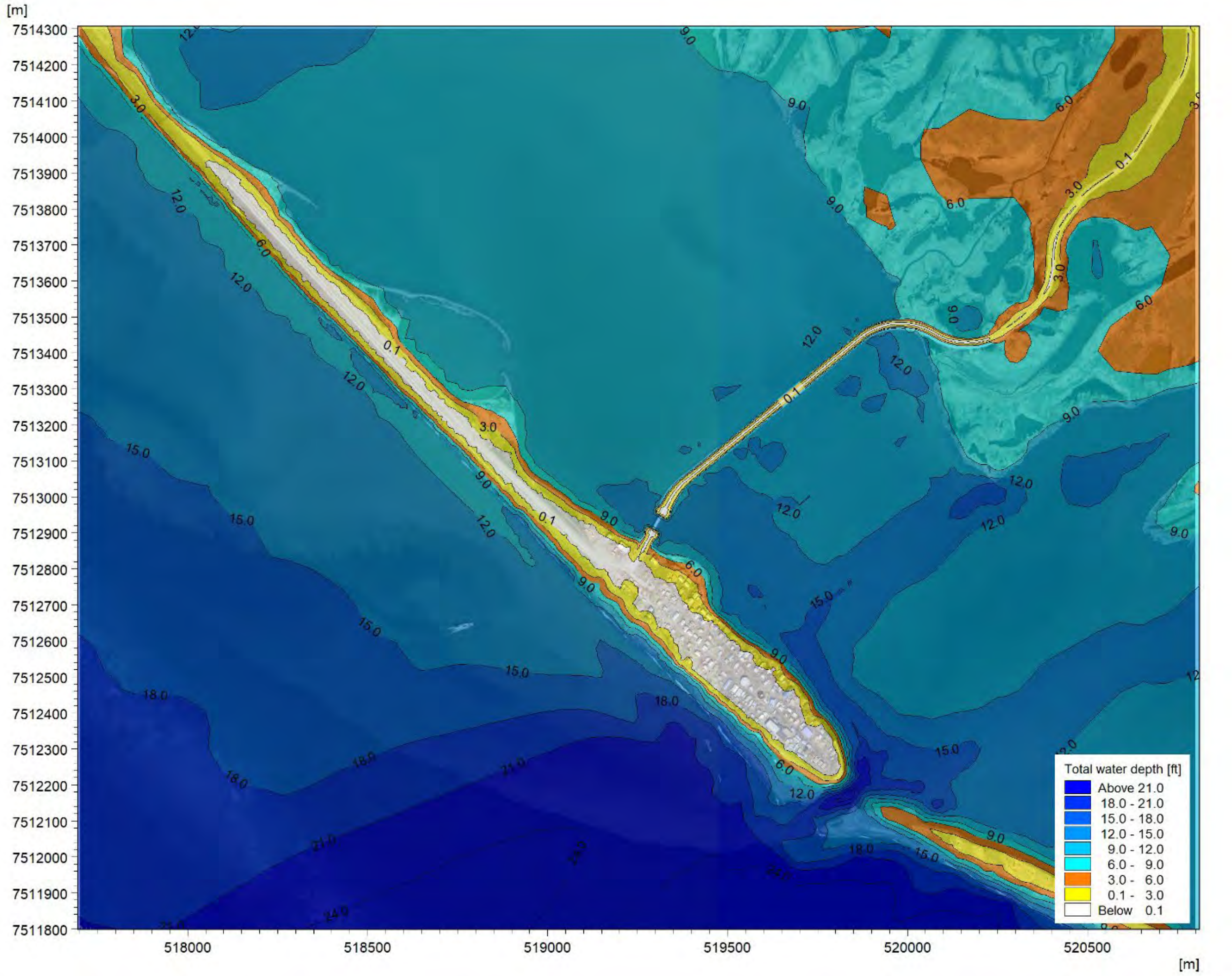

Figure A-8: Maximum Water Depth for 100 Year Event at SLR 2050 (HDSW_C14)

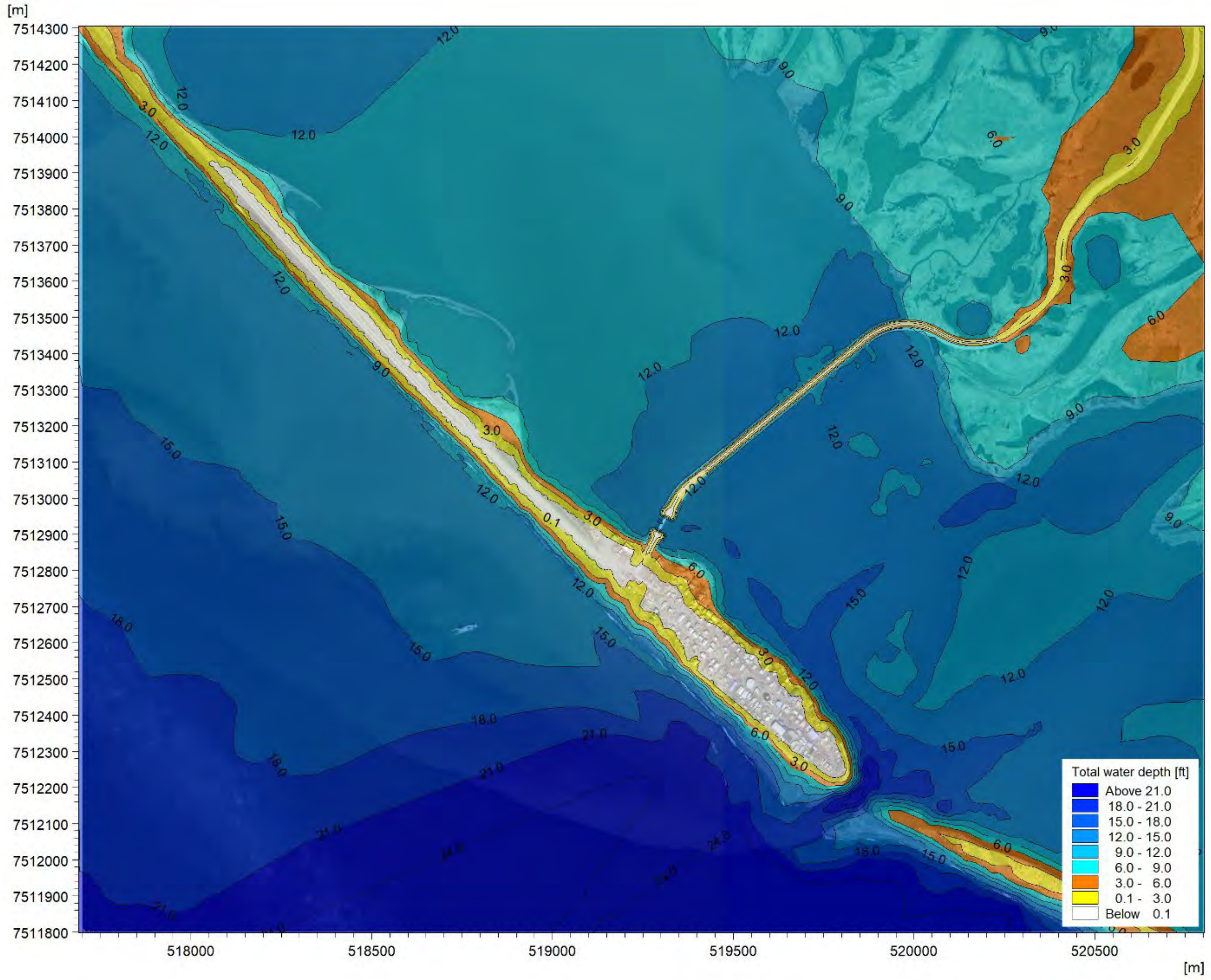

Figure A-9: Maximum Water Depth for 10 Year Event at SLR 2075 (HDSW_C21)

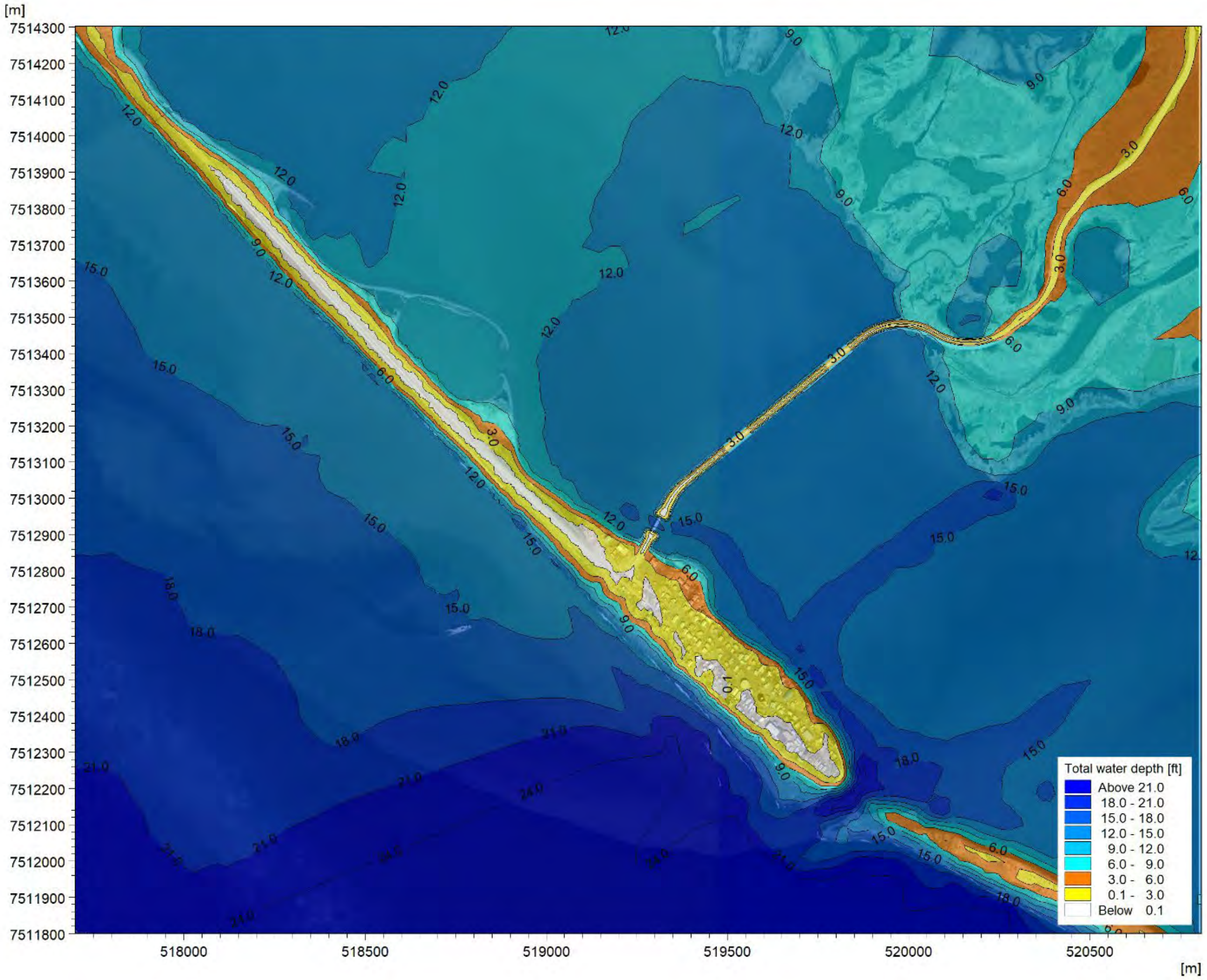

Figure A-10: Maximum Water Depth for 25 Year Event at SLR 2075 (HDSW_C22)

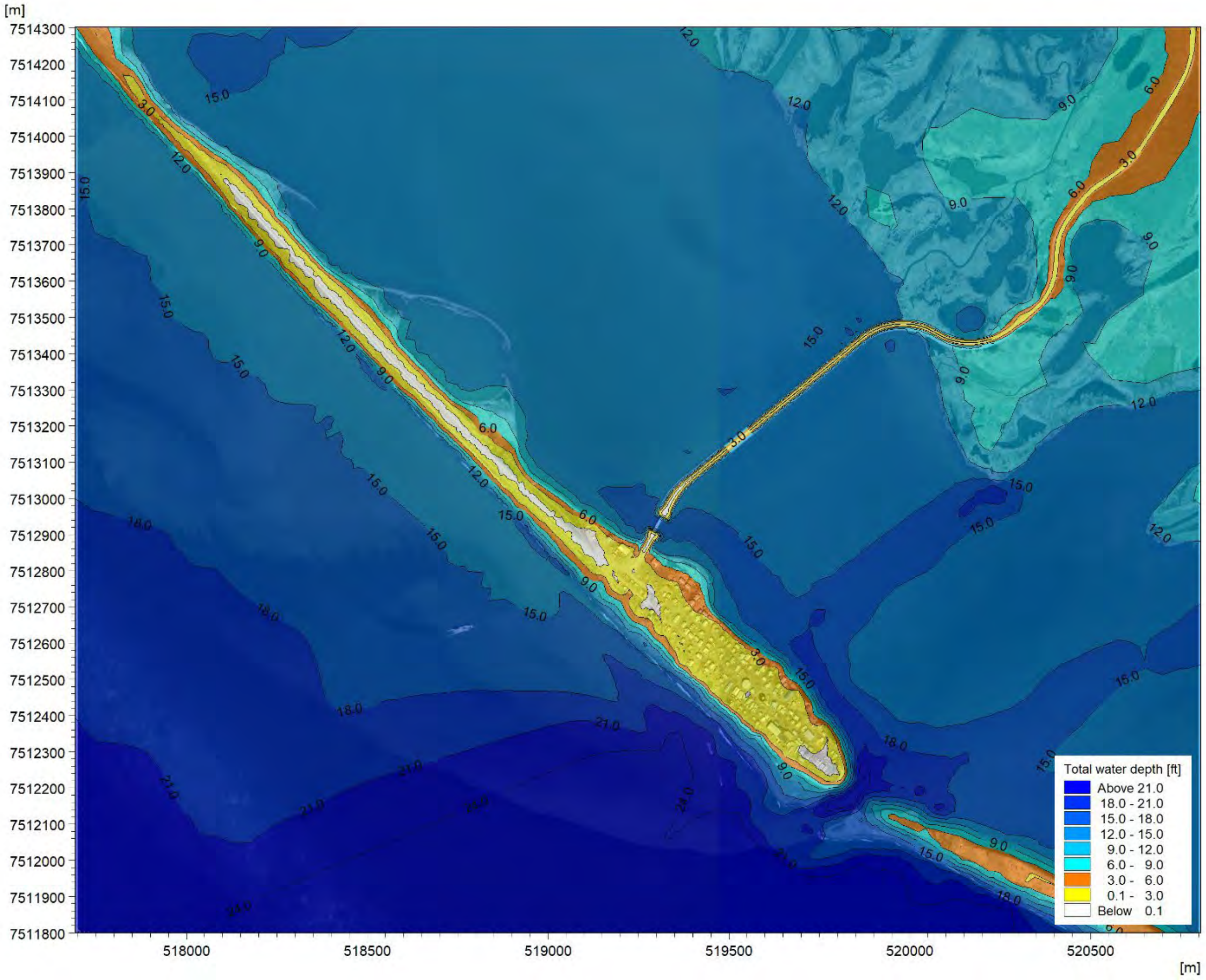

Figure A-11: Maximum Water Depth for 50 Year Event at SLR 2075 (HDSW_C23)

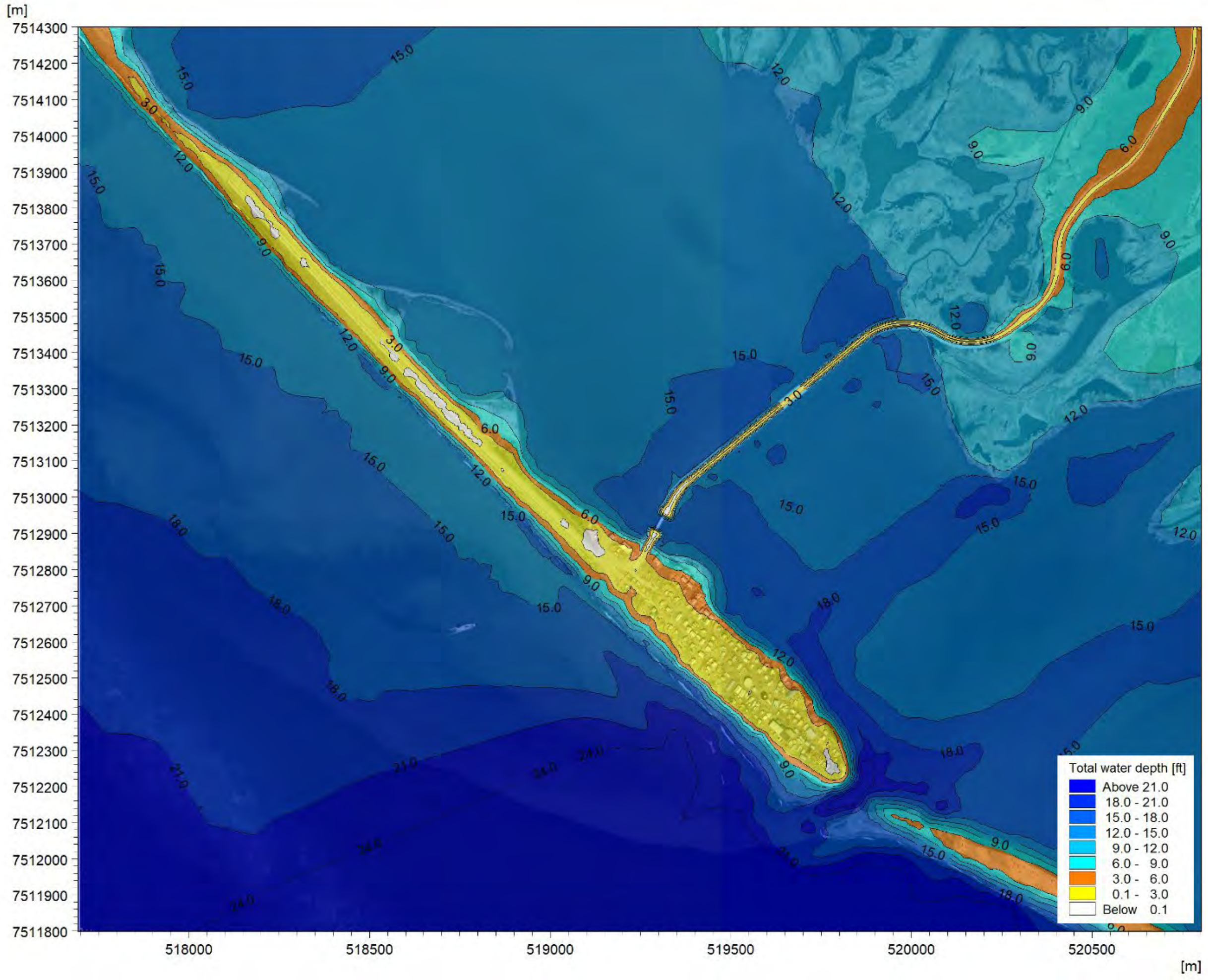

Figure A-12: Maximum Water Depth for 100 Year Event at SLR 2075 (HDSW_C24)

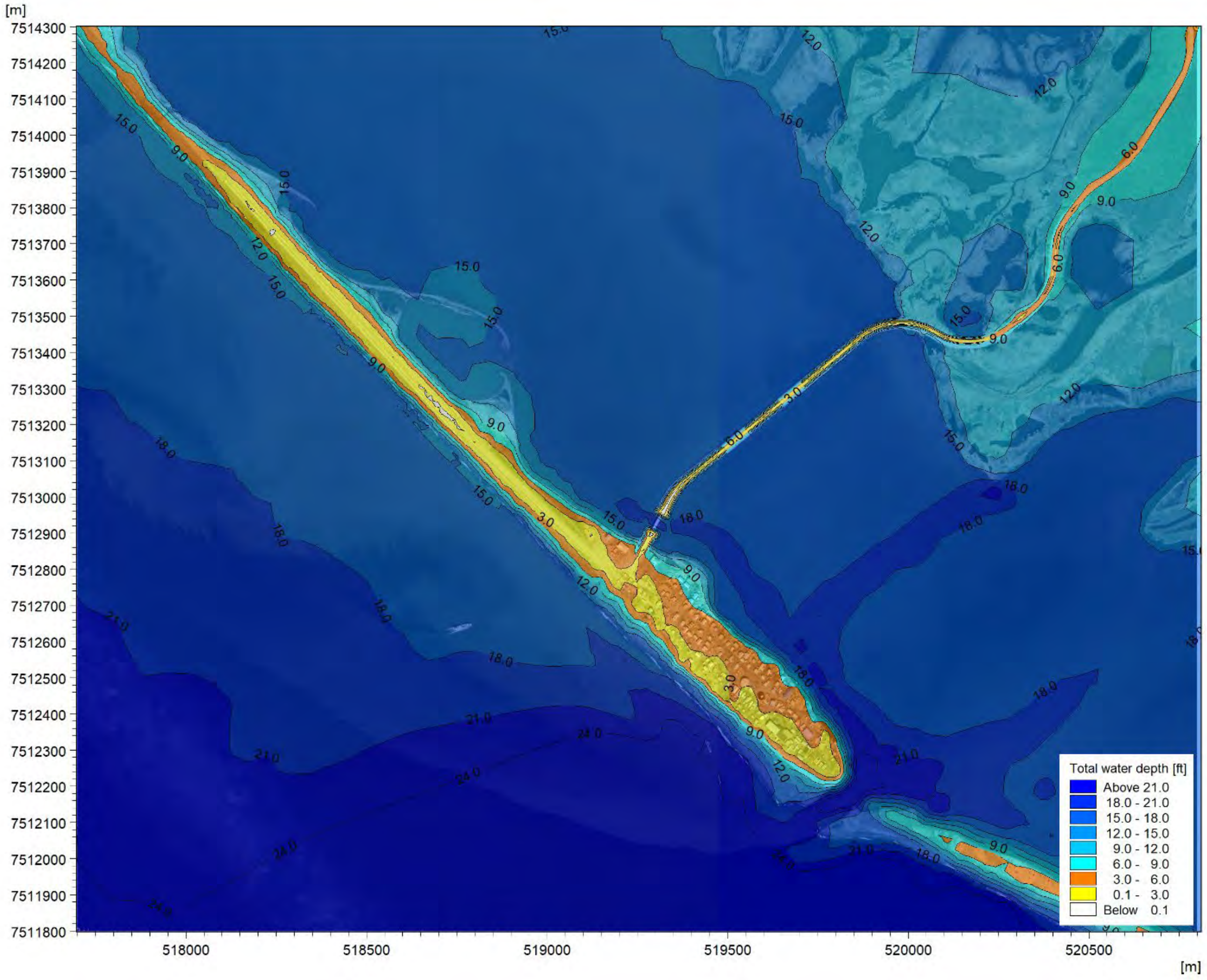

Figure A-13: Maximum Water Depth for 10 Year Event at SLR 2100 (HDSW_C31)

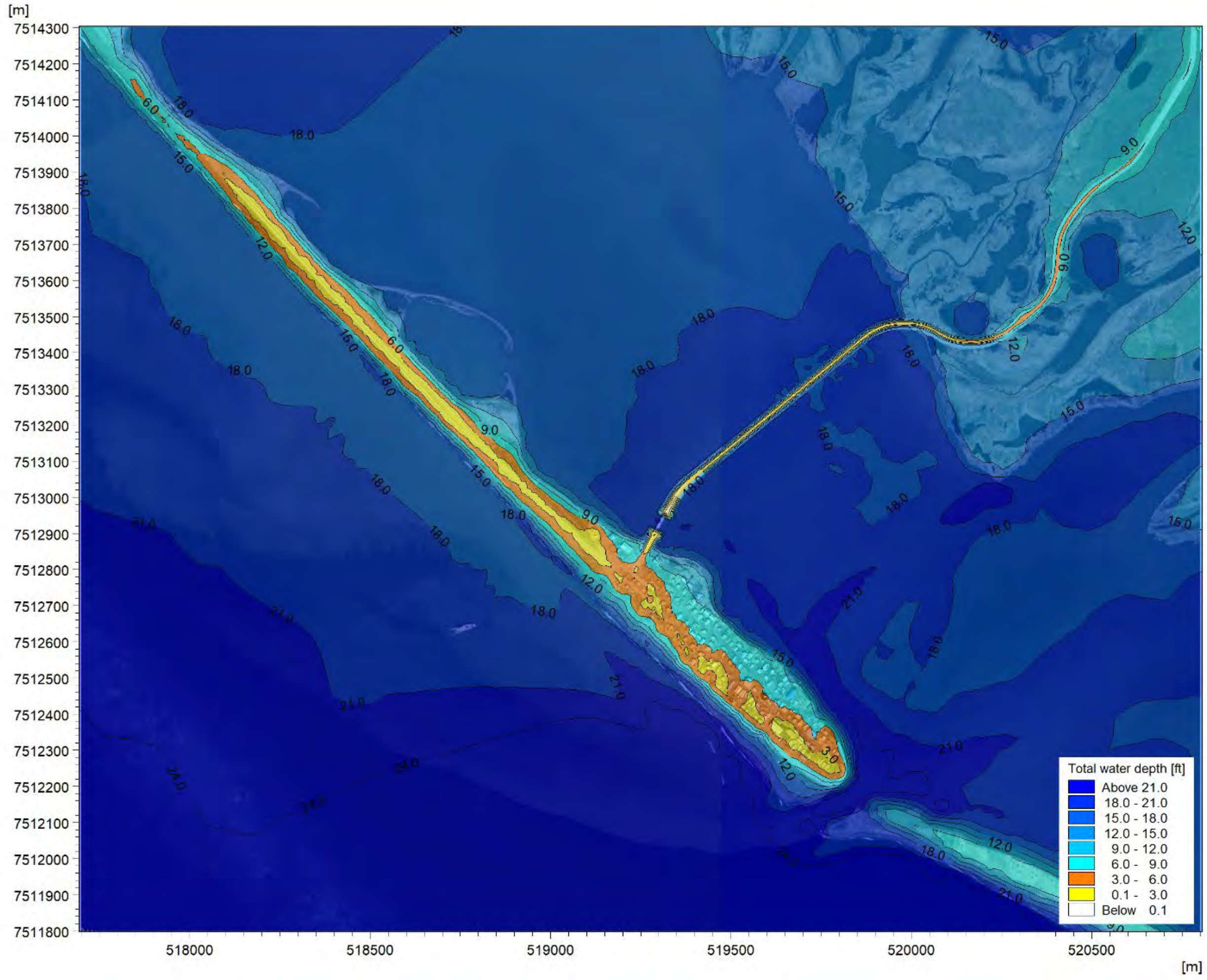

Figure A-14: Maximum Water Depth for 25 Year Event at SLR 2100 (HDSW_C32)

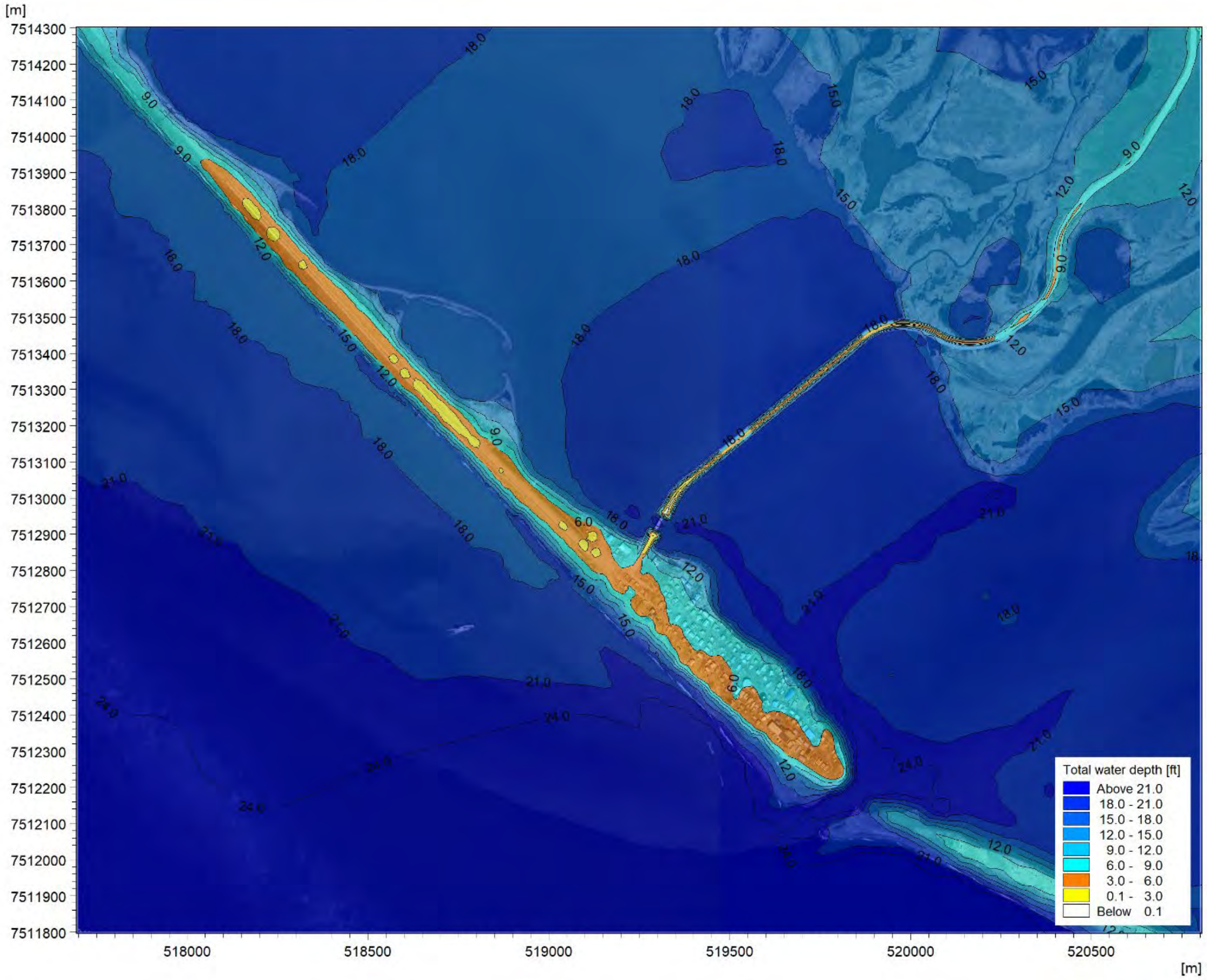

Figure A-15: Maximum Water Depth for 50 Year Event at SLR 2100 (HDSW_C33)

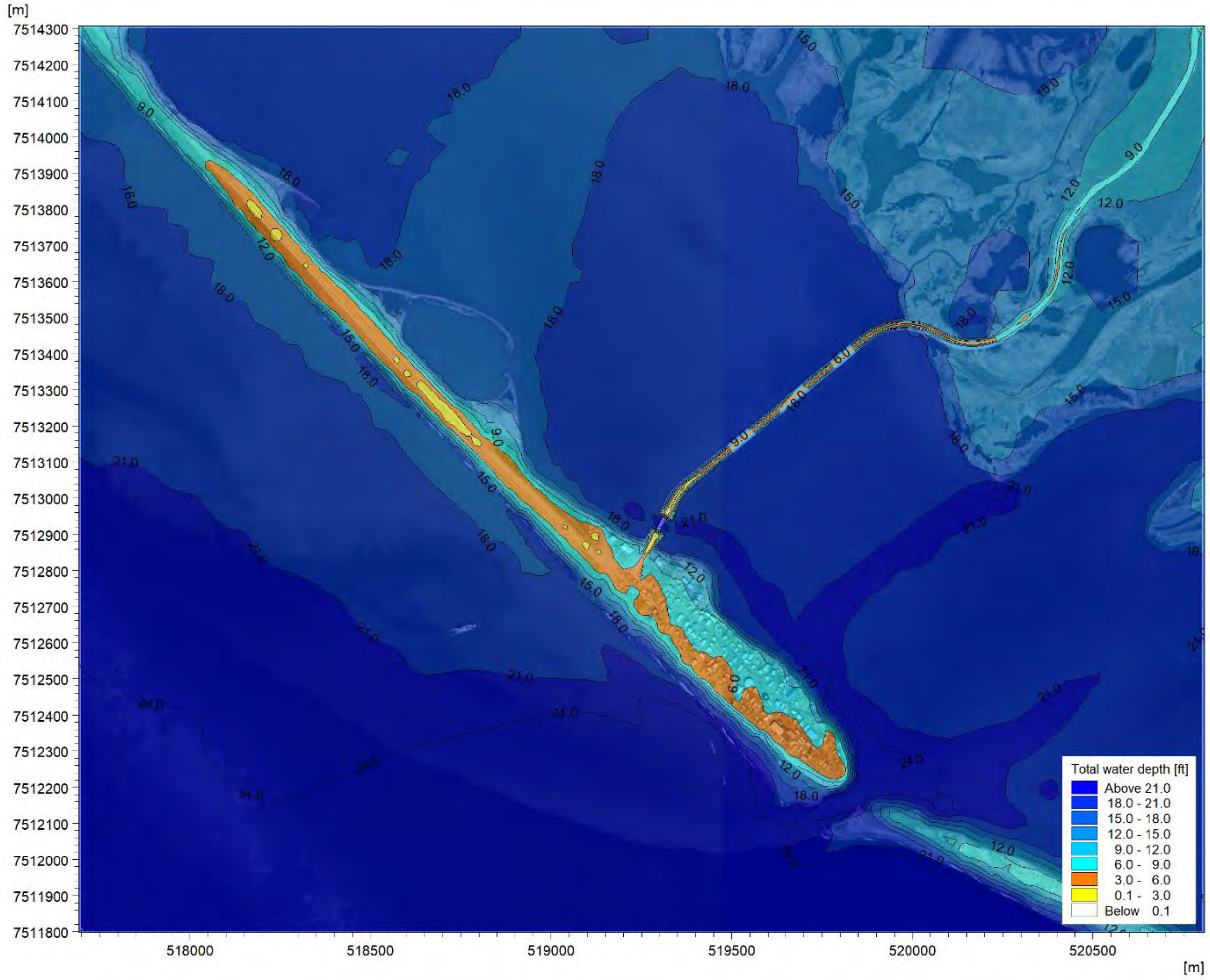

Figure A-16: Maximum Water Depth for 100 Year Event at SLR 2100 (HDSW_C34)

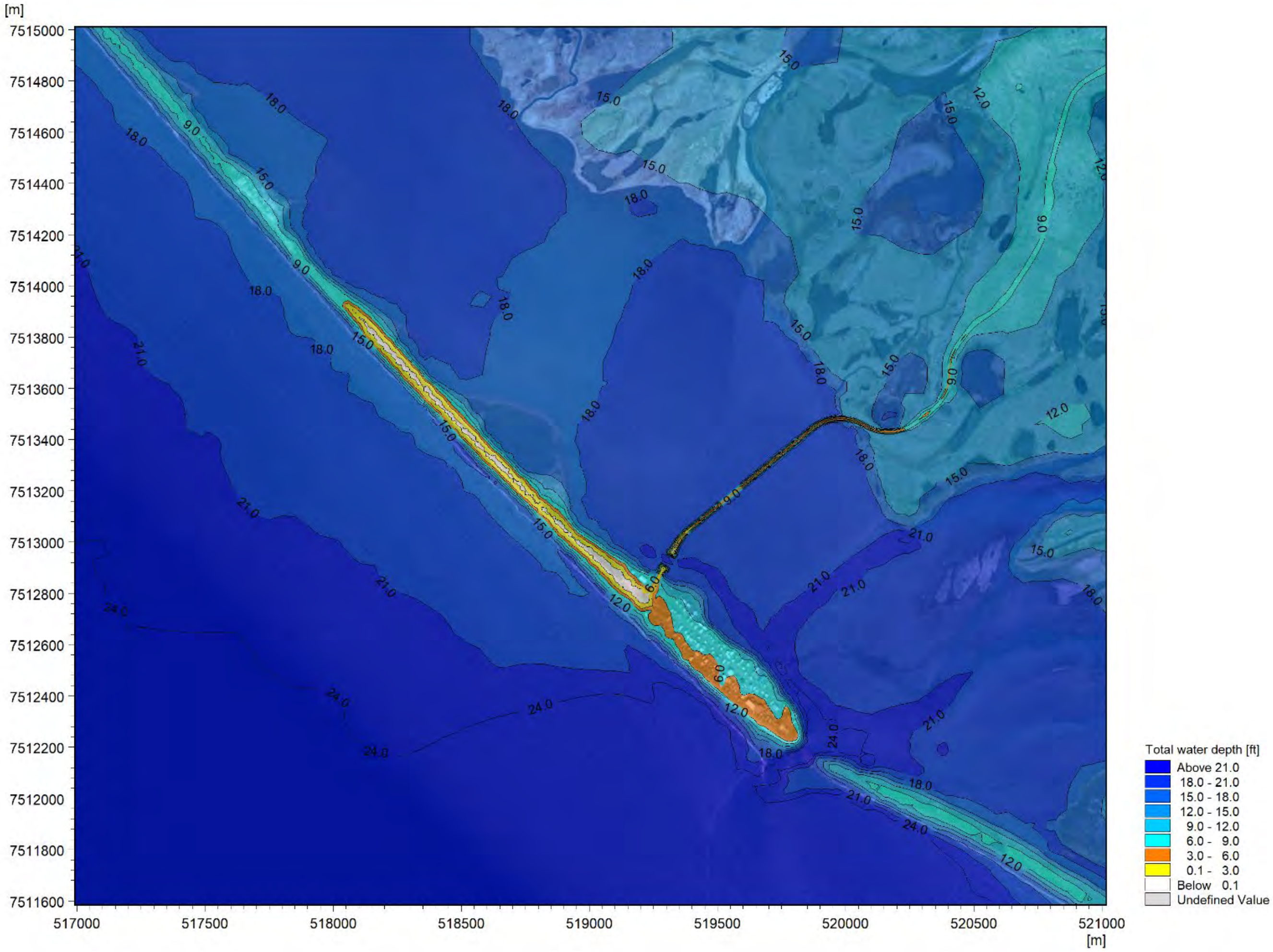

Figure A-17: Maximum Water Depth for 100 Year Event at SLR 2100 with raised runway elevation of 21 ft NAVD88 (HDSW_C35)